

A non-radial two-body collapse model (TBCM) for gravitational collapse of dark matter in
expanding background and generalized stable clustering hypothesis (GSCH)

Zhijie (Jay) Xu^{1,a}

1. Computational Mathematics Group, Physical and Computational Sciences Directorate, Pacific
Northwest National Laboratory, Richland, WA 99352, USA

Abstract:

Analytical tools are valuable to study the self-gravitating collisionless flow in expanding background (SG-CFD). However, it is extremely hard to find analytical solutions for highly non-linear structure formation. Only a few simple but powerful tools exist so far. Two examples are the spherical collapse model (SCM) and stable clustering hypothesis (SCH). This paper presents another analytical tool based on an elementary step of halo mass accretion/cascade, i.e. a two-body collapse model (TBCM). The TBCM model plays the same role as simple harmonic oscillator model in dynamics. Just like the importance and ubiquity of harmonic oscillator, the TBCM model can be fundamental to understand the self-gravitating collisionless flow.

Instead of expanding background, the TBCM model is equivalently formulated for gravity with an arbitrary power-law exponent n in a transformed system with static background and fixed damping. Depending on the exponent n , Hubble constant H_0 , and initial separation and velocity, the competition between gravity, expanding background (damping), and angular momentum classifies two-body collapse into two categories: a free fall collapse without oscillatory motion (weak angular momentum) and an equilibrium collapse (weak damping) that persists much longer in time with oscillations. For free fall collapse, the free fall time in expanding background depends

a) Electronic mail: zhijie.xu@pnnl.gov; zhijiexu@hotmail.com

on the ratio of free fall time in static background (s_c) to the beginning time of free fall (t_i). Free fall time is greater if the same two-body system starts to collapse at an earlier time (smaller t_i).

For equilibrium collapse, perturbative solutions demonstrate an exponential evolution of system size, energy, and momentum in transformed system, or equivalently power-law evolution in original comoving system. Two critical values (β_{s1} and β_{s2}) can be identified that quantifies the competition between damping and gravity. The first value $\beta_{s1}=1$ is identified from the existence of an equilibrium range. The second value $\beta_{s2}=1/(3\pi)$ is identified from the existence of halos with infinitesimal lifetime (extremely fast mass accretion). The critical value β_{s2} only exists for a set of discrete values of potential exponent $n = (2 - 6m)/(1 + 3m) = -1, -10/7, -8/5 \dots$ and so on to -2 for integer m . The critical density ratio of $18\pi^2$ can be obtained from β_{s2} for the special case $n=-1$ that is surprisingly consistent with SCM model.

The TBCM model predicts the two-body angular velocity scales as $\omega_r \sim Hr^{-3/2}$ with the separation r ; The angle θ_{vr} between particle velocity and particle position satisfies $\cot(\theta_{vr}) = -\beta_{s2}$ for halos with infinitesimal lifetime. Halo energies can be obtained without using halo density, where the isothermal density is shown to be a direct result of infinitesimal lifetime. The TBCM model demonstrates the stable clustering hypothesis (SCH) for equilibrium collapse, where the mean pairwise velocity (first moment) $\langle \Delta u_L \rangle = -Hr$. A generalized stable clustering hypothesis (GSCH) can be developed for higher order moments $\langle \Delta u_L^{2m+1} \rangle = (2m+1) \langle \Delta u_L^{2m} \rangle \langle \Delta u_L \rangle$. The two-body collapse in expanding background is independent of particle mass, where energy equipartition does not apply. Compared to the spherical collapse model (SCM), TBCM model can be naturally considered as a spherical non-radial collapse model with non-zero angular momentum.

Both models predict the same critical halo density ratio of $18\pi^2$, while the TBCM model contains much richer information for gravitational collapse of collisionless matter.

Key word: Gravitational Collapse, Collisionless Flow, Spherical Collapse, Stable Clustering, Dark Matter Halos

Contents

Nomenclature	5
1. Introduction	6
2. Equations of motion for comoving and transformed systems	8
3. Analytical solutions for TBCM in expanding background	11
3.1 Analytical formulation of a TBCM model.....	11
3.2 Numerical solutions and three distinct regimes for TBCM	17
3.3 Free fall collapse and free fall time in expanding background	22
3.4 TBCM model in the simplest form and perturbative solutions for equilibrium collapse.....	27
3.5 Critical values of β_s for equilibrium collapse and critical density	32
3.6 Solutions for energy, virial quantity, and angular momentum.....	37
3.7 The two-body angular velocity ω_t , critical angle θ_{vr} , and halo kinetic energy	40
4. Connections with existing theories.....	44
4.1 Connections with stable clustering hypothesis (SCH) and generalized SCH	44
4.2 Connections with violent relaxation	48
4.3 Connections with spherical collapse model (SCM).....	49
5. Conclusion.....	52

Nomenclature

See supplementary information

1. Introduction

Collisionless systems often show properties strongly suggesting common physical principles that control the system motion and evolution. The self-gravitating collisionless fluid dynamics (SG-CFD) is the study of motion of collisionless matter under its own gravity. The large-scale gravitational collapse is an example of SG-CFD, which forms the basis of standard models for the formation of large-scale structures. Structure formation starts from the gravitational collapse of small-scale density fluctuations and proceeds hierarchically in a “bottom-up” fashion with small structures merging into large structures. The same process can be described by a halo-mediated inverse mass cascade, where halos (the building blocks) pass their mass onto larger and larger halos, until halo mass growth becomes dominant over mass propagation [1]. Halos are necessary to form for collisionless system with long-range interaction to maximize system entropy [2]. The merging of halos is an elementary step during this process and a focus of current paper.

The hierarchical merging of structures is fundamental and complex for structure formation. In a finite interval Δt of time, the hierarchical merging might involve multiple substructures merging into a single large structure. However, for an infinitesimal interval dt , that process should involve the merging of two and only two substructures. In this regard, the two-body gravitational collapse is an elementary and fundamental step for hierarchical structure formation. While the two-body problem in static background (no space expansion) without damping is well-known, a comprehensive understanding of the two-body collapse (TBCM) in expanding background seems not fully developed. In fact, the TBCM model can be a powerful analytical tool to study the non-linear structure formation and provide many insights into the energy and momentum evolution at large scale. This is made possible with analytical solutions by transforming the original two-body system in expanding background to the same system in static background but with a fixed damping.

Results obtained in transformed system can be equivalently translated back to the original comoving system.

Despite the great success of large-scale N -body simulations for structure formation, there are always motivations for finding analytical approaches to gravitational collapse. However, it can be extremely hard to find analytical solutions for highly non-linear structure formation problem. Nonetheless, a few simple but powerful analytical tools exist for structure evolution. The first example makes use a spherical symmetry of an over-density to formulate the gravitational collapse, i.e. a spherical collapse model (SCM). Developed by Gunn & Gott [3] and Gunn [4] in 1970s, the first SCM model provides solutions for the collapse of a spherical mass shell surrounding an over-density with an uniform density. The self-similar spherical collapse model was later developed in 1980s to allow for a non-uniform initial density and collapse of new shells [5, 6]. The idea of SCM model was further developed to consider the effect of non-radial orbit by introducing an additional constant centrifugal force due to the non-radial motion [7, 8].

The second example assumes that on a sufficiently small scale, the clusters of mass particles are bound and stable with a fixed mean physical separation between particles, i.e. a stable clustering hypothesis (SCH) [9, 10]. There is no stream motion between particles in physical coordinate. In this sense, the peculiar motion cancels out the Hubble flow and the hypothesis equivalently states that the mean (first order moment) pairwise peculiar velocity is proportional to the separation r (physical distance) as $\langle \Delta u_L \rangle = -Hr$. The stable clustering hypothesis is a fundamental assumption for the nonlinear gravitational collapse at small scales. Combined with pair conservation equation [11], the hypothesis can be used to predict the dynamic evolution of density correlation function on small scales. There have been many attempts to verify this

assumption with N -body simulations [12, 13], while the limited resolution of simulations makes it difficult to achieve a sufficiently high accuracy at small scales where this assumption is valid.

In this paper, a two-body collapse model (TBCM) model is developed to provide an additional analytical tool and more insights into the structure formation and evolution. The TBCM model is able to demonstrate the standard stable clustering hypothesis on small scale for the first moment of pairwise velocity. A generalized stable clustering hypothesis (GSCH) can be derived for high order moments. The connections of TBCM with violent relaxation and spherical collapse model (SCM) are also discussed. The rest of the paper is organized as follows: Section 2 introduces the equations of motion for the dynamics of a N -body system. Equivalence is established between the original comoving system in expanding background and a transformed system in static background. The elementary gravitational collapse (TBCM model) is formulated and analytically solved in Section 3, along with the applications of TBCM to identify distinct regimes and critical values. Connections with stable clustering hypothesis, violent relaxation and spherical collapse models are discussed in Section 4.

2. Equations of motion for comoving and transformed systems

In this section, the equivalence is first established between a comoving system in expanding background and a transformed system in static background. The self-gravitating of a system of N collisionless particles in expanding background can be studied by solving governing equation of motion [11] (page 44) in a comoving system (comoving coordinates \mathbf{x} and physical time t) as

$$\frac{d^2 \mathbf{x}_i}{dt^2} + 2H \frac{d\mathbf{x}_i}{dt} = -\frac{Gm_p}{a^3} \sum_{j \neq i}^N \frac{\mathbf{x}_i - \mathbf{x}_j}{|\mathbf{x}_i - \mathbf{x}_j|^3}, \quad (1)$$

where \mathbf{x}_i is the comoving coordinate of N particles with equal mass m_p and G is the standard gravitational constant. The Hubble constant $H(t) = \dot{a}/a$, where a is the scale factor.

For halos with a growing size from mass accretion, an effective gravitational potential exponent $n_e \approx -1.3$ (different from -1) can be shown due to the finite halo surface energy (Eq. (96) in [14]). This hints the necessity of looking at a general potential with an arbitrary exponent n . The maximum entropy distributions of velocity and energy in SG-CFD have been developed for the long-range power-law potential with any exponent n in [M3]. In this paper, we assume the same power-law gravitational potential V_p with an arbitrary exponent of n for particle-particle interacting, i.e. $V_p(r) = -G_n m_p^2 / r^{-n}$. Here G_n is a generalized gravitational constant ($G_n = G$ when $n = -1$). The equation of motion with arbitrary exponent n reads

$$\frac{d^2 \mathbf{x}_i}{dt^2} + 2H \frac{d\mathbf{x}_i}{dt} = \frac{nG_n m_p}{a^3} \sum_{j \neq i}^N \frac{\mathbf{x}_i - \mathbf{x}_j}{|\mathbf{x}_i - \mathbf{x}_j|^{2-n}}. \quad (2)$$

Let's introduce a new transformed time scale s as $ds/dt = a^p$, where p is an arbitrary exponent.

The original Eq. (2) can be equivalently transformed to

$$\frac{d^2 \mathbf{x}_i}{ds^2} + \frac{d\mathbf{x}_i}{ds} (p+2) a^{-p} H = \frac{nG_n m_p}{a^{3+2p}} \sum_{j \neq i}^N \frac{\mathbf{x}_i - \mathbf{x}_j}{|\mathbf{x}_i - \mathbf{x}_j|^{2-n}}. \quad (3)$$

Obviously $s = t$ if $p = 0$ and Eq. (3) is reduced to Eq. (2). Specifically, $p = -2$ eliminates the first order derivative and s is the time variable for integration of N -body simulation that allows for a symplectic (phase space volume preserving) integrator. Time scale s becomes conformal time if $p = -1$. Another special case can be identified with $p = -3/2$ and Einstein-de Sitter (EdS) matter-dominant model,

$$H_0^2 = H^2 a^3, \quad \frac{dH}{dt} = -\frac{3}{2}H^2, \quad \text{and} \quad H^2 = \frac{8\pi G \bar{\rho}_y(a)}{3}, \quad (4)$$

where H_0 is the Hubble constant at the present epoch ($a=1$) and $\bar{\rho}_y(a)$ is the physical density of the homogeneous background. For $p = -3/2$ with Eq. (4), equation (Eq. (3)) becomes

$$\frac{d^2 \mathbf{x}_i}{ds^2} + \frac{1}{2} H_0 \frac{d\mathbf{x}_i}{ds} = n G_n m_p \sum_{j \neq i}^N \frac{\mathbf{x}_i - \mathbf{x}_j}{|\mathbf{x}_i - \mathbf{x}_j|^{2-n}} = \frac{\mathbf{F}_i}{m_p}, \quad (5)$$

where \mathbf{F}_i is the resultant force on particle i in comoving system. Clearly, the scale factor a does not appear in Eq. (5) and the Hubble constant H_0 can be considered as a constant damping that is time-invariant. The original Eq. (2) in expanding background is now equivalently converted to a transformed system in static background with a constant damping $H_0/2$ (Eq. (5)) evolving with a new time scale s . The transformed system consists of a comoving spatial coordinate \mathbf{x}_i and a transformed time scale s . The particle velocity \mathbf{v}_i for transformed system can be written as,

$$\mathbf{v}_i = \frac{d\mathbf{x}_i}{ds} = a^{3/2} \frac{d\mathbf{x}_i}{dt} = a^{1/2} \mathbf{u}_i, \quad (6)$$

while the peculiar velocity \mathbf{u}_i in the physical time t can be related to the new velocity \mathbf{v}_i ,

$$\mathbf{u}_i = a \frac{d\mathbf{x}_i}{dt} = \frac{d\mathbf{r}_i}{dt} - H\mathbf{r}_i = a^{-1/2} \mathbf{v}_i, \quad (7)$$

where $\mathbf{r}_i = a\mathbf{x}_i$ is the physical coordinate of particle i .

In this section, the original equation of motion (Eq. (2)) for a comoving system in expanding background is equivalently transformed to Eq. (5) for a transformed system with a constant damping in static background. While two systems are essentially equivalent, analytical solutions can be more accessible in the transformed system for convenience.

3. Analytical solutions for TBCM in expanding background

The two-body gravitational collapse is a fundamental and elementary process. Halos are often created by two-body collapse of two smaller halos with either comparable masses or very different masses (for example, halos merging with a single merger). By this mean, halos pass their mass to larger and larger halos such that two-body gravitational collapse is an elementary step for inverse mass cascade [1] and halo mass accretion. Therefore, it should be very instructive to solve a simple two-body collapse model (TBCM) in expanding background.

3.1 Analytical formulation of a TBCM model

Solutions are well-known for two-body problem in a static background without damping. Here we focus on the two-body collapse in expanding background. Again, the two-body interaction is assumed to have a general power-law form with an exponent n . We first solve the TBCM model in transformed system (static background with a constant damping) for convenience. Results can be readily transformed back to the original comoving system.

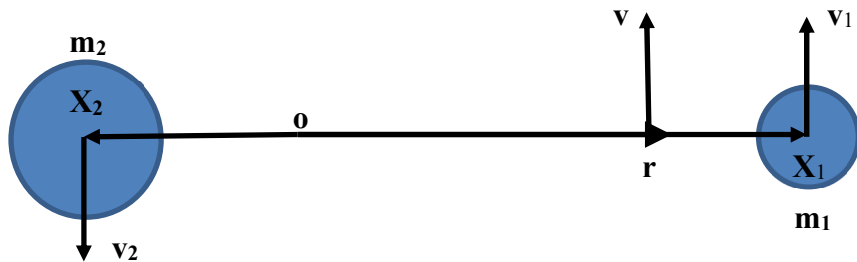


Figure 1. Schematic plot of a two-body gravitational collapse in expanding background. The two-body system consists of two masses m_1 and m_2 with a separation of $2r$, where r is the displacement vector. Here v_1 , v_2 and v are the velocities of two masses and the displacement vector, respectively.

As shown in Fig. 1, the two-body system of two masses m_1 and m_2 with a separation of $2r$ in expanding background can be equivalently described by following equations in the transformed system (from Eq. (5)),

$$\ddot{\mathbf{x}}_1 + \frac{H_0}{2} \dot{\mathbf{x}}_1 = \frac{nG_n m_2}{(2r)^{1-n}} \cdot \frac{\mathbf{r}}{|\mathbf{r}|}, \quad (8)$$

$$\ddot{\mathbf{x}}_2 + \frac{H_0}{2} \dot{\mathbf{x}}_2 = -\frac{nG_n m_1}{(2r)^{1-n}} \cdot \frac{\mathbf{r}}{|\mathbf{r}|}, \quad (9)$$

where \mathbf{x}_1 and \mathbf{x}_2 are position vectors of two masses and $\mathbf{v}_j = \dot{\mathbf{x}}_j$ ($j=1, 2$) is the velocity in transformed system with time derivative with respect to s . The displacement vector is defined as $\mathbf{r} = (\mathbf{x}_1 - \mathbf{x}_2)/2$ and r is the magnitude of vector \mathbf{r} . The equation of motion for the center of mass can be obtained by multiplying Eqs. (8) and (9) with m_1 and m_2 , respectively, and adding them together,

$$\ddot{\mathbf{R}} + \frac{H_0}{2} \dot{\mathbf{R}} = 0, \quad (10)$$

where $\mathbf{R} = (m_1 \mathbf{x}_1 + m_2 \mathbf{x}_2)/(m_1 + m_2)$ is the position vector of the center of mass. Similarly, the equation for displacement vector \mathbf{r} can be obtained by subtracting Eq. (9) from Eq. (8),

$$\ddot{\mathbf{r}} + \frac{H_0}{2} \dot{\mathbf{r}} = \frac{nG_n (m_1 + m_2)}{2(2r)^{1-n}} \cdot \frac{\mathbf{r}}{|\mathbf{r}|}, \quad (11)$$

The position vectors of two masses can be expressed in terms of \mathbf{r} and \mathbf{R} as

$$\mathbf{x}_1 = \mathbf{R} + 2m_2 \mathbf{r}/(m_1 + m_2) = \mathbf{R} + \mu \mathbf{r},$$

where $\mu = 2m_2/(m_1 + m_2)$ is a dimensionless constant, and

$$\mathbf{x}_2 = \mathbf{R} - 2m_1 \mathbf{r}/(m_1 + m_2) = \mathbf{R} - (2 - \mu) \mathbf{r}. \quad (12)$$

We assume a fixed center of mass at the origin o (see Fig. 1) such that $\mathbf{R} = 0$ and Eq. (10) is trivial by properly choosing the initial positions and velocities of two masses. The dynamics of the original problem is now reduced to the motion of a point mass subject to gravity and a constant damping $H_0/2$ (Eq. (11)).

Since two-body motion is planar, let's try a general solution for the displacement vector \mathbf{r} in the x - y plane, where the cartesian components of displacement vector \mathbf{r} and its velocity \mathbf{v} read

$$x = r(s) \cos(\omega(s)s) \text{ and } y = r(s) \sin(\omega(s)s), \quad (13)$$

$$v_x = \dot{x} = \dot{r} \cos(\omega s) - r \sin(\omega s)(\omega + s\dot{\omega})$$

and

$$v_y = \dot{y} = \dot{r} \sin(\omega s) + r \cos(\omega s)(\omega + s\dot{\omega}). \quad (14)$$

Both radius $r(s)$ and the frequency term $\omega(s)$ are functions of time s . From Eq. (12), the position and velocity of two masses can be related to that of the displacement vector \mathbf{r} as

$$\mathbf{x}_1 = \mu \mathbf{r} \quad \text{and} \quad \mathbf{x}_2 = -(2 - \mu) \mathbf{r}, \quad (15)$$

$$\mathbf{v}_1 = \mu \dot{\mathbf{r}} \quad \text{and} \quad \mathbf{v}_2 = -(2 - \mu) \dot{\mathbf{r}}. \quad (16)$$

For example, the position (\mathbf{x}_1) and velocity vectors (\mathbf{v}_1) of mass m_1 in x - y plane can be found as,

$$x_1 = \mu r(s) \cos(\omega s) \text{ and } y_1 = \mu r(s) \sin(\omega s) \quad (17)$$

$$v_{x1} = \mu v_x = \mu \dot{r} \cos(\omega s) - \mu r \sin(\omega s)(\omega + s\dot{\omega})$$

and

$$v_{y1} = \mu v_y = \mu \dot{r} \sin(\omega s) + \mu r \cos(\omega s)(\omega + s\dot{\omega}). \quad (18)$$

The initial positions of two masses m_1 and m_2 are set as

$$r_1(s=0) = |\mathbf{x}_{i1}| = \mu r_i, \quad r_2(s=0) = |\mathbf{x}_{i2}| = (2 - \mu) r_i, \quad (19)$$

where $r_i = r(s=0)$ is the magnitude of the displacement vector \mathbf{r} , \mathbf{x}_{i1} and \mathbf{x}_{i2} are the initial position vectors of two masses. The initial velocities of masses m_1 and m_2 can be set as,

$$v_{x1}(s=0) = 0 \text{ and } v_{y1}(s=0) = v_{i1} = \mu v_i, \quad (20)$$

$$v_{x2}(s=0) = 0 \text{ and } v_{y2}(s=0) = v_{i2} = -(2-\mu)v_i, \quad (21)$$

where v_i is the initial velocity of the displacement vector \mathbf{r} in y direction. These initial conditions satisfy a zero linear momentum with $m_1 v_{i1} + m_2 v_{i2} = 0$. Obviously, $\mathbf{R} = 0$ is a trivial solution for Eq. (10) with these initial conditions (Eqs. (19) and (20)).

A special case is that the initial speed v_i of displacement vector satisfies

$$v_i = v_{ri} = \sqrt{\frac{-nG_n r_i}{(2r_i)^{1-n}} \frac{m_1 + m_2}{2}}, \quad (22)$$

where the corresponding speeds of two masses v_{i1} and v_{i2} are

$$\frac{v_{i1}^2}{|\mathbf{x}_{i1}|} = \frac{-nG_n m_2}{(2r_i)^{1-n}} \quad \text{and} \quad \frac{v_{i2}^2}{|\mathbf{x}_{i2}|} = \frac{-nG_n m_1}{(2r_i)^{1-n}}. \quad (23)$$

Here v_{ri} is the circling velocity of the displacement vector \mathbf{r} if there is no damping. For this special case, the two-body system is stable with both masses circling around the center of mass if the background is static ($H_0 = 0$). More specifically, the initial system is in a virial equilibrium ($2KE - nPE = 0$) with

$$v_i^2 = v_{ri}^2 = \alpha_s \frac{G_n (m_1 + m_2)}{r_i^{-n}} = \alpha_s \frac{G_n M}{r_i^{-n}}, \quad (24)$$

where constant $\alpha_s = -n/2^{2-n}$ and $M = m_1 + m_2$ is the total mass of the system. Without loss of generality, we will try to solve the two-body collapse problem with an arbitrary initial velocity v_i

for displacement vector \mathbf{r} . Substituting the assumed solution (Eq. (13)) into Eq. (11) gives rise to two coupled equations for two unknown functions: radius $r(s)$ and frequency $\omega(s)$,

$$\underbrace{\ddot{r}}_1 + \underbrace{\frac{H_0}{2}\dot{r}}_2 - \underbrace{\frac{nG_n(m_1+m_2)}{2(2r)^{1-n}}}_{2} = \underbrace{r(\omega+s\dot{\omega})^2}_3 = r\left(\frac{\partial(\omega s)}{\partial s}\right)^2, \quad (25)$$

$$\frac{\dot{r}}{r} = -\frac{1}{2}\left[\frac{\partial \ln(\omega+s\dot{\omega})}{\partial s} + \frac{H_0}{2}\right]. \quad (26)$$

with initial conditions,

$$r|_{s=0} = r_i \text{ and } \left(\frac{\partial r}{\partial s}\right)|_{s=0} = 0. \quad (27)$$

Three forces contribute to the equation of motion for $r(s)$ in Eq. (25), i.e. the damping force (term 1), the gravitational force (term 2), and the frequency force (term 3). Term 3 (frequency force) originates from the angular momentum as we will show in Eq. (30). The competition among three forces dominates the evolution of $r(s)$. Let's now introduce a frequency function as

$$F(s) = (\omega+s\dot{\omega})^{-1/2} = \left(\frac{\partial(\omega s)}{\partial s}\right)^{-1/2}. \quad (28)$$

The radius $r(s)$ can be obtained by solving Eq. (26),

$$r(s) = (r_i v_i)^{1/2} F(s) \exp\left(-\frac{1}{4}H_0 s\right). \quad (29)$$

A single equation for radius function $r(s)$ can be easily obtained by substitution of Eq. (29) for frequency function $F(s)$ into Eq. (25),

$$\ddot{r} + \frac{H_0}{2}\dot{r} - \frac{nG_n(m_1+m_2)}{2(2r)^{1-n}} = \frac{(r_i v_i)^2}{r^3} \exp(-H_0 s). \quad (30)$$

The frequency force (term 3 in Eq. (25)) is now related to the initial angular momentum ($r_i v_i$ on the right hand side (RHS)) and is exponentially decaying with time s . Complete solution of Eq. (30) depends on five parameters, i.e. the exponent n , damping H_0 , initial conditions r_i and v_i , and system mass $M = m_1 + m_2$. This equation mimics the spherical collapse model (SCM) but with a non-zero angular momentum on the RHS. Comparison is discussed in Section 4.3.

However, Eq. (30) is complex to solve analytically. Here we take a different route by directly solving the frequency function $F(s)$ (instead of $r(s)$ in Eq. (30)), where five parameters can be grouped into exponent n and two dimensionless numbers (Eqs. (60) and (61)). Equations (25) and (26) are first combined and rewritten in terms of the frequency function $F(s)$,

$$\frac{\ddot{r}}{r} + \frac{H_0}{2} \frac{\dot{r}}{r} + \frac{v_{ri}^2}{r^2} \left(\frac{r}{r_i} \right)^n = F^{-4}(s), \quad (31)$$

$$\frac{\dot{r}}{r} = \frac{1}{F(s)} \frac{\partial F}{\partial s} - \frac{H_0}{4}. \quad (32)$$

With the identity

$$\frac{\ddot{r}}{r} = \frac{\partial(\dot{r}/r)}{\partial s} + \left(\frac{\dot{r}}{r} \right)^2, \quad (33)$$

substitution of Eq. (32) into Eq. (31) leads to a single differential equation for frequency function

$F(s)$ (no first order derivative involved):

$$\frac{\partial^2 F}{\partial s^2} = \underbrace{\frac{H_0^2}{16} F(s)}_1 - \underbrace{\gamma_s \left(\frac{v_i}{r_i} \right)^{1+n/2} F^{n-1}(s) \exp\left(-\frac{n-2}{4} H_0 s \right)}_2 + \underbrace{F^{-3}(s)}_3 \quad (34)$$

with initial conditions:

$$F(s=0) = \left(\frac{r_i}{v_i}\right)^{1/2} \quad \text{and} \quad \left.\frac{\partial F}{\partial s}\right|_{s=0} = \frac{H_0}{4} \left(\frac{r_i}{v_i}\right)^{1/2} \quad \text{from (Eq. (27)),} \quad (35)$$

where $\gamma_s = (v_{ri}/v_i)^2$ is a dimensionless number indicating how far the initial system is away from virial equilibrium (the special case in (Eq. (22))). $\gamma_s = 1$ corresponds to the special case with initial system in virial equilibrium.

With function $F(s)$ fully determined by the Eq. (34) and the initial condition (35), the radius $r(s)$ and frequency $\omega(s)$ can be solved subsequently using Eqs. (29) and (28). Similarly, three terms (1, 2 and 3) on the RHS of Eq. (34), i.e. the damping force, the gravitational force, and the frequency force (from angular momentum), contribute to the evolution of $F(s)$.

3.2 Numerical solutions and three distinct regimes for TBCM

Exact solution of highly nonlinear Eq. (34) is still not available in a closed form. However, numerical solutions can be easily obtained. Figure 2 shows typical trajectories of displacement vector \mathbf{r} in x - y plane for three different $n = -0.5, -1.0,$ and -1.5 . The trajectories are for the gravitational collapse of two masses in a transformed system. Initial systems are in virial equilibrium, where displacement vector \mathbf{r} simply circles around the origin if $H_0 = 0$. The trajectory becomes very complex for systems with different potential exponent n and a nonzero damping ($H_0 \neq 0$ for expanding background).

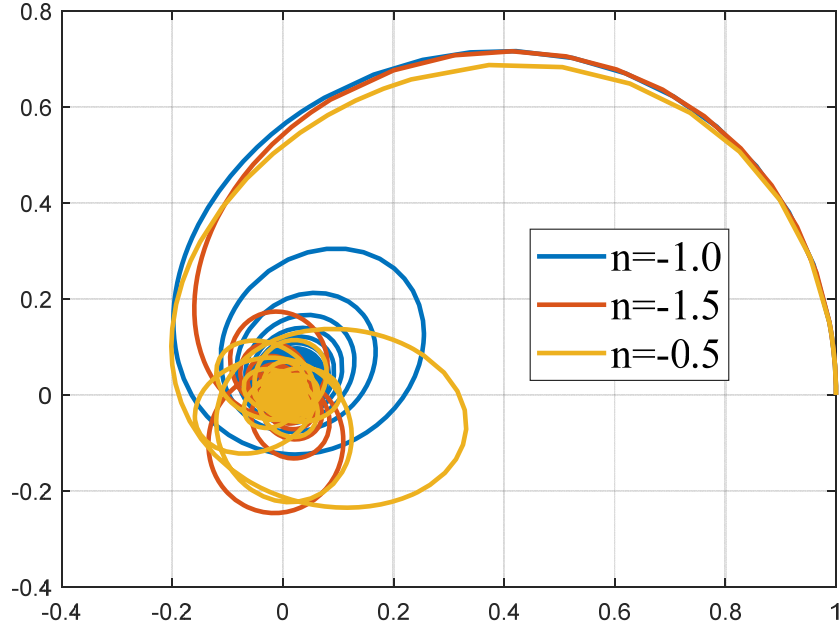


Figure 2. The trajectory of the displacement vector \mathbf{r} in x - y plane for three different n with $H_0 = 0.4$, $G_n M = 1$, $r_i = 1$ and $\gamma_s = 1$ (or $v_i = v_{r_i}$), i.e. the initial system is in virial equilibrium. The trajectory becomes very complex for systems with different potential exponents n and a nonzero damping ($H_0 \neq 0$ stands for expanding background).

The time evolutions of the specific kinetic, potential, and total energy for the same three cases are presented in Figure 3, where both kinetic and potential energies of two-body system (K_s and P_s) vibrate around their mean values before the final collapse. The oscillation cancels out for total energy $E_s = K_s + P_s$, which is relatively smooth. A smaller exponent n tends to have a longer time span of oscillation and smaller oscillation amplitude. More detailed discussion of energy evolution and their solutions is presented in Section 3.6.

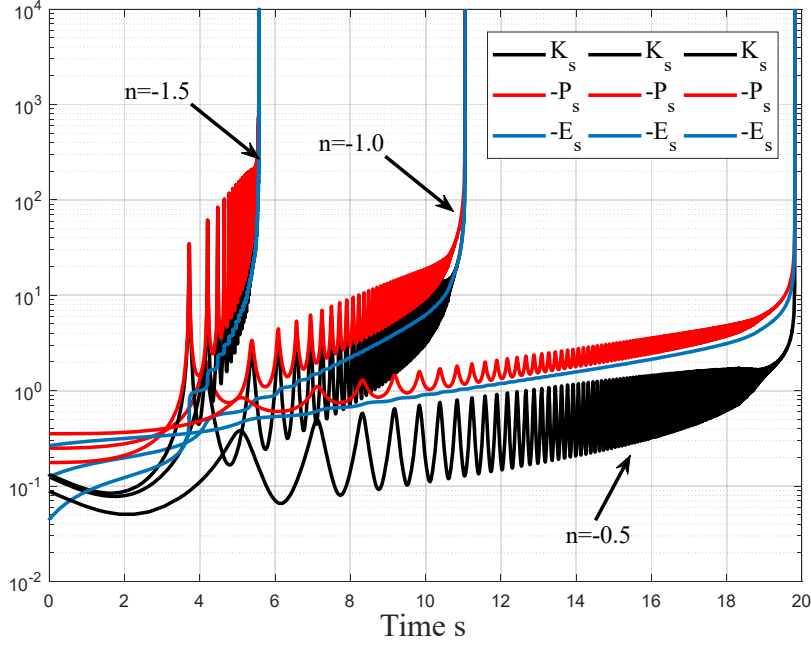


Figure 3. The temporal evolution of energy for a two-body gravitational collapse for three different exponents n with $H_0 = 0.4$, $G_n M = 1$, $r_i = 1$ and $\gamma_s = 1$ (or $v_i = v_{ri}$). Both kinetic and potential energy (K_s and P_s) vibrate around their mean values before the final collapse. The oscillation cancels out for the total energy $E_s = K_s + P_s$. A smaller exponent n tends to have a longer time span of oscillation and smaller amplitude of oscillation.

Figure 4 presents typical trajectories for four different scenarios, depending on a dimensionless number $\lambda_s = H_0 r_i / (4v_i)$ and the exponent n . All scenarios have $\gamma_s = 1$ or $v_i = v_{ri}$, i.e. the special case considered in Eq. (22). The periodic motion only exists for small λ_s and $-2 < n < 0$. The dimensionless number λ_s quantifies the competition between gravity and damping, while the ratio $\gamma_s = (v_{ri}/v_i)^2$ quantifies the competition between gravity and angular momentum. There exists a critical value of λ_s for the existence of periodic motion that we will identify later.

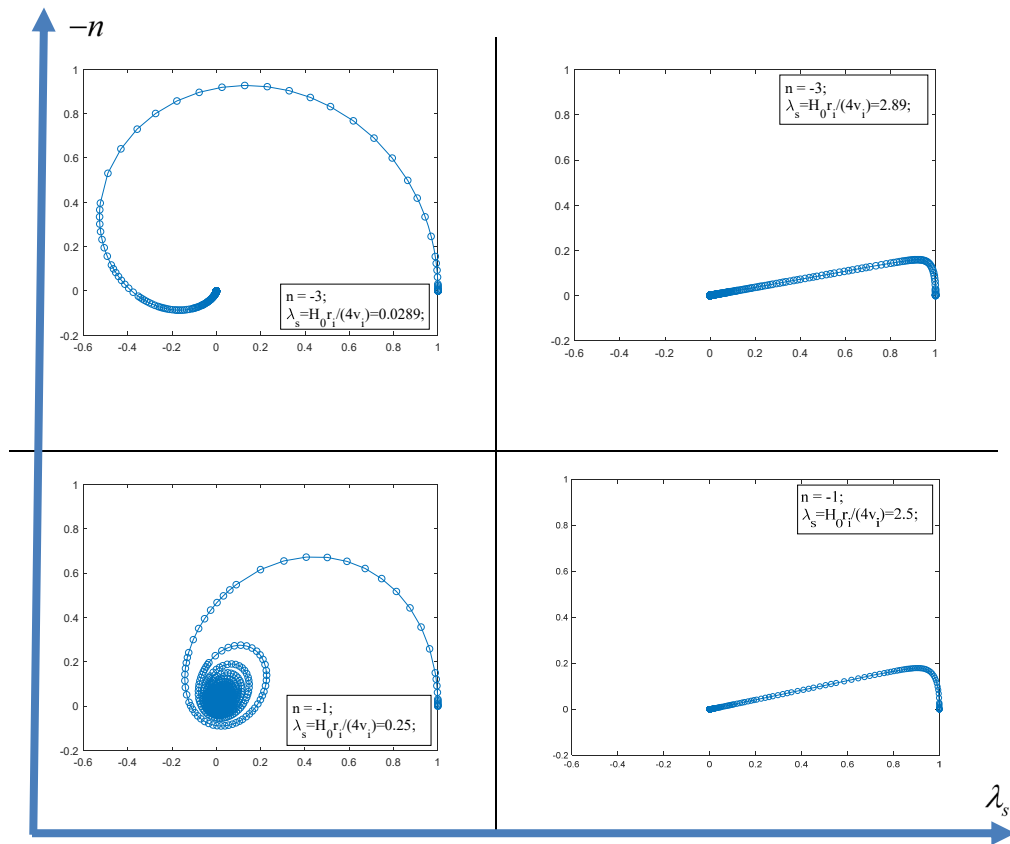


Figure 4. Four typical trajectories for different combinations of parameter λ_s and potential exponent n with $\gamma_s = 1$. The oscillatory motion only exists for small λ_s (weak damping) and $-2 < n < 0$. The critical value of λ_s for an oscillatory motion will be identified.

Figure 5 shows the time variation of the radius function $r(s)$ of displacement vector for the same four scenarios. Three distinct regimes can be identified for an equilibrium collapse (green line), i.e. an initial transitional range dominated by the damping force, an equilibrium range dominated by the competition between the gravitational and the frequency forces, and a final collapse. System spends most time in the equilibrium range if an oscillating motion exists.

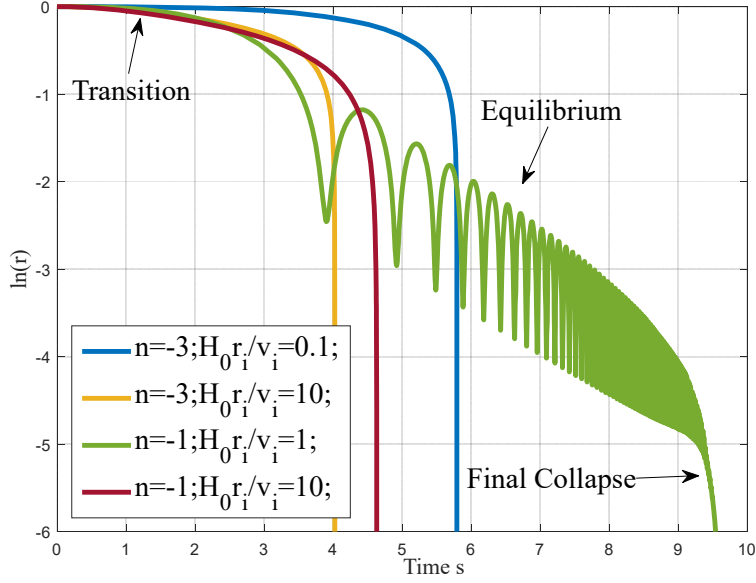


Figure 5. The temporal evolution of the radius $r(s)$ with time s for four cases presented in Fig. 4. For an equilibrium collapse with oscillating motion, three distinct ranges can be identified, an initial transition range dominated by the damping force, an equilibrium range dominated by the competition between the gravitational and the frequency forces, and a final collapse. The equilibrium collapse only exists for weak damping with a small λ_s , $-2 < n < 0$, and $\gamma_s \approx 1$.

Term 1 (damping) on the RHS of Eq. (34) can be dominant over the other two terms initially.

The solution of $F(s)$ for the transition range can be found as,

$$F(s) = \left(\frac{r_i}{v_i}\right)^{1/2} \exp\left(\frac{H_0 s}{4}\right) \text{ and } r(s) = r_i. \quad (36)$$

Since term 1 (damping) is dominant at the transition range, we have (from Eq. (34)),

$$\frac{H_0^2}{16} F(s_t) = \left| \gamma_s \left(\frac{v_i}{r_i}\right)^{1+n/2} F^{n-1}(s_t) \exp\left(-\frac{n-2}{4} H_0 s_t\right) - F^{-3}(s_t) \right| \quad (37)$$

to define a transition time s_t . After substitution of Eq. (36) into Eq. (37), we have

$$\lambda_s^2 = \left| \gamma_s - \exp(-H_0 s_t) \right|, \quad (38)$$

where the dimensionless number λ_s is defined as $\lambda_s = H_0 r_i / (4v_i)$ and the transition time s_t is dependent on λ_s and γ_s . Damping force is dominant for $t < s_t$.

For equilibrium range, term 2 (gravitational force) approximately balances the term 3 (the frequency force) which leads to a mean frequency function $F_m(s)$ from Eq. (34),

$$F_m(s) = \gamma_s^{-1/(2+n)} \left(\frac{r_i}{v_i} \right)^{1/2} \exp\left(-\frac{2-n}{2+n} \cdot \frac{H_0 s}{4} \right). \quad (39)$$

The actual solution $F(s)$ vibrates around the mean solution $F_m(s)$. The mean solutions for the radius and frequency can be found using Eqs. (29) and (28),

$$r_m(s) = \gamma_s^{-1/(2+n)} r_i \exp\left(-\frac{H_0 s}{2+n} \right), \quad (40)$$

$$\omega_m(s) = \frac{1}{2\lambda_s} \frac{2+n}{2-n} \gamma_s^{2/(2+n)} \exp\left(\frac{2-n}{2+n} \cdot \frac{H_0 s}{2} \right). \quad (41)$$

Actual radius and frequency solutions should also vibrate about mean solutions (Fig. 5).

3.3 Free fall collapse and free fall time in expanding background

The free fall time is the characteristic time it takes for two-body to collapse under their own gravity. The TBCM model can be used to estimate the free fall time in expanding background. For small initial velocity with $v_i \rightarrow 0$ (vanishing angular momentum) or large exponent n ($v_{ri} \rightarrow \infty$ from Eq. (22)), the parameter $\gamma_s = (v_{ri}/v_i)^2 \rightarrow \infty$. This is the free fall of a test particle from rest at an initial distance of r_i with a fixed damping. Term 2 (gravitational force) in Eq. (34) should be dominant for free fall and the solution of $F(s)$ is approximately a parabolic function without oscillatory motion. From Eq. (34) and initial condition in Eq. (35), equation for $F(s)$ reads

$$\frac{\partial^2 F}{\partial s^2} \approx -\gamma_s \left(\frac{v_i}{r_i} \right)^{1+n/2} F^{n-1}(s=0) = -\gamma_s \left(\frac{v_i}{r_i} \right)^{3/2}. \quad (42)$$

With initial conditions in Eq. (35), the approximate solution of Eq. (42) is

$$F(s) \approx \left(\frac{r_i}{v_i} \right)^{1/2} \left[-\frac{1}{32} \left(\frac{H_0}{\lambda_{si}} \right)^2 s^2 + \frac{1}{4} H_0 s + 1 \right], \quad (43)$$

where parameter (quantifies the competition of gravity with damping for free fall collapse)

$$\lambda_{si} = \frac{H_0 r_i}{4 v_{ri}} = \lambda_s \gamma_s^{-1/2} = \frac{\lambda_s v_i}{v_{ri}} = H_0 \sqrt{\frac{2^{-n-2} r_i^{2-n}}{-n G_n (m_1 + m_2)}}. \quad (44)$$

The radius function of displacement vector can be found from Eq. (29),

$$r(s) \approx r_i \exp\left(-\frac{1}{4} H_0 s\right) \left[-\frac{1}{32} \left(\frac{H_0}{\lambda_{si}} \right)^2 s^2 + \frac{1}{4} H_0 s + 1 \right]. \quad (45)$$

The final collapse (free fall) time s_c in time scale s can be estimated by setting $r(s = s_c) = 0$,

$$s_c \approx \frac{4 \lambda_{si}^2}{H_0} \left[1 + \sqrt{1 + \frac{2}{\lambda_{si}^2}} \right]. \quad (46)$$

For small λ_{si} ($r_i \rightarrow 0$, or weak damping $H_0 \rightarrow 0$, or $M \rightarrow \infty$) in Eq. (44), s_c is essentially the free fall time in static background without damping (from Eq. (46)),

$$s_c \approx s_{c1} = 4\sqrt{2} \frac{\lambda_{si}}{H_0} = \sqrt{2} \frac{r_i}{v_{ri}} = \sqrt{\frac{2^{3-n} r_i^{2-n}}{-n G_n (m_1 + m_2)}} = \frac{\sqrt{2}}{2\pi} T_{ri}, \quad (47)$$

which does not depend on the damping H_0 . Here T_{ri} is the orbital period,

$$T_{ri} = \frac{2\pi r_i}{v_{ri}} = \frac{2\pi (2r_i)^{1-n/2}}{\sqrt{-n G_n (m_1 + m_2)}}. \quad (48)$$

Specifically, for $n = -1$, we have

$$s_{c1} = \frac{4r_i^{3/2}}{\sqrt{G(m_1 + m_2)}} = \frac{\sqrt{2}}{2\pi} T_{ri}, \quad (49)$$

which well approximates the exact free fall time s_{ce} in static background without damping, where

$$s_{ce} = \frac{\pi r_i^{3/2}}{\sqrt{G(m_1 + m_2)}} = \frac{\sqrt{2}}{8} T_{ri} \quad (50)$$

is the exact free fall time in static background. Note that s_{c1} is obtained from approximation Eq. (42) and cannot reduce to exact free fall time s_{ce} .

While for large λ_{si} ($r_i \rightarrow \infty$, or strong damping $H_0 \rightarrow \infty$, or $M \rightarrow 0$) in Eq. (44), the free fall time is proportional to the damping H_0 ,

$$s_c \approx s_{c2} = 8 \frac{\lambda_{si}^2}{H_0} = \frac{H_0 r_i^2}{2v_{ri}^2} = \frac{H_0}{8\pi^2} T_{ri}^2 = \frac{H_0 2^{1-n} r_i^{2-n}}{-nG_n(m_1 + m_2)}. \quad (51)$$

The critical value between two regimes can be obtained from Eqs. (47) and (51) with $s_{c1} = s_{c2}$, where $\lambda_{si} = \sqrt{2}/2$. The free fall time from Eq. (46) approximates the true free fall time in transformed system. Figure 6 plots the variation of free fall time (normalized by H_0) with the dimensionless number λ_{si} . The comparison between the numerical solution by solving the original Equation (Eqs. (8) and (9)) and approximation Eq. (46) justifies a correction factor λ_c ,

$$s_c = 4\lambda_c \frac{\lambda_{si}^2}{H_0} \left[1 + \sqrt{1 + \frac{2}{\lambda_{si}^2}} \right],$$

where the correction factor

$$\lambda_c = \frac{\pi}{4} \text{ for } \lambda_{si} \rightarrow 0 \text{ and } \lambda_c = \frac{1}{3} \text{ for } \lambda_{si} \rightarrow \infty. \quad (52)$$

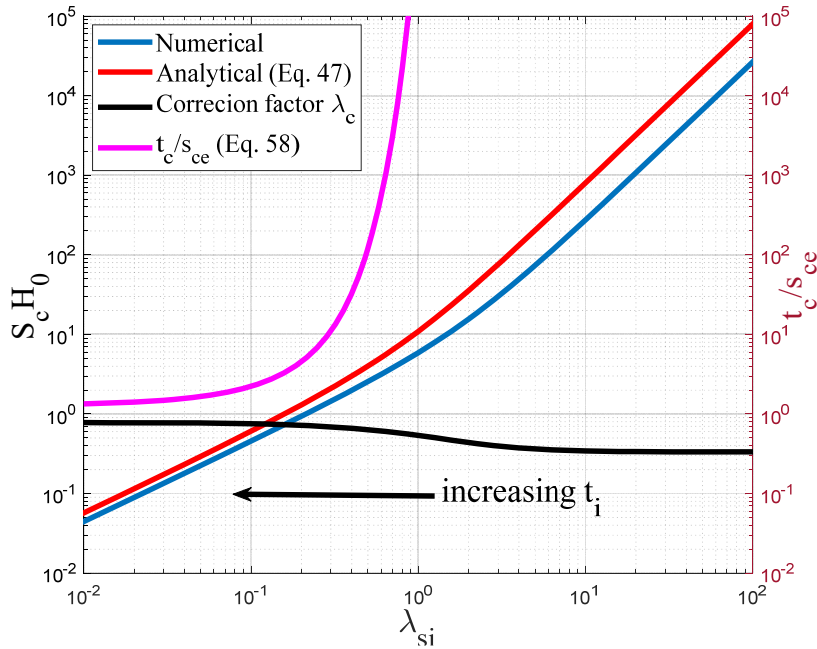


Figure 6. The variation of free fall time s_c (normalized by H_0) with dimensionless number λ_{si} . The comparison between numerical solution by solving the original equation of motion and the analytical approximation is also presented. The ratio between two is plotted as the correction factor λ_c . The free fall time s_c (in transformed system with static background and fixed damping) is proportional to damping H_0 for large λ_{si} . The variation of the physical free fall time t_c (normalized by the free fall time s_{ce} that is for static background and no damping) with λ_{si} is also plotted on the right axis, which increases with λ_{si} . The two-body system starting to collapse at an earlier time will have a longer free fall time. Time t_c approaches s_{ce} when s_{ce} is small (small separation or large mass) or when collapse time t_i approaches t_0 .

Note that s_c is the free fall time in transformed system. To transform it back to the original comoving system, the relation between two time scales t and s ($ds/dt = a^{-3/2}$) is

$$s = t_0 \ln(t/t_i) \quad \text{and} \quad t_e = t_i \exp(s_c/t_0), \quad (53)$$

where $t_i = a_i^{3/2} t_0$ and t_e are the start and end of a two-body free fall in physical time t , a_i is the scale factor at initial time t_i . Here t_0 is the present physical time with $H_0 t_0 = 2/3$. The free fall time ($t_c = t_e - t_i$) for a two-body system to fully collapse in expanding background is,

$$t_c = t_i \left(\exp \left(\frac{s_c}{t_0} \right) - 1 \right) \approx \frac{t_i s_c}{t_0}. \quad (54)$$

Let's consider a two-body system with an initial separation of $2r_{yi}$ in physical coordinates, the exact free fall time for such a two-body system in static background without damping should be (same as Eq. (50), but in a physical coordinate $r_{yi} = a_i r_i$),

$$s_{ce} = \frac{\pi r_{yi}^{3/2}}{\sqrt{G(m_1 + m_2)}}. \quad (55)$$

For $n = -1$, the dimensionless λ_{si} can be rewritten in terms of the ratio s_{ce}/t_i from Eq. (44),

$$\lambda_{si} = H_0 \frac{(r_{yi}/a_i)^{3/2}}{\sqrt{2G_n(m_1 + m_2)}} = \frac{\sqrt{2}}{3\pi} \frac{s_{ce}}{t_i}. \quad (56)$$

The free fall time in the original comoving system is given by (from Eqs. (54), (52), and (56))

$$\begin{aligned} \frac{t_c}{s_{ce}} &= \frac{\sqrt{2}}{3\pi\lambda_{si}} \left(\exp \left[6\lambda_c \lambda_{si}^2 \left(1 + \sqrt{1 + \frac{2}{\lambda_{si}^2}} \right) \right] - 1 \right) \\ &= \frac{t_i}{s_{ce}} \left(\exp \left[\frac{4\lambda_c}{3\pi^2} \left(\frac{s_{ce}}{t_i} \right)^2 \left(1 + \sqrt{1 + 9\pi^2 \left(\frac{t_i}{s_{ce}} \right)^2} \right) \right] - 1 \right). \end{aligned} \quad (57)$$

where two regimes can be clearly identified as,

$$t_c = \frac{4}{\pi} \lambda_c s_{ce} \text{ for } \lambda_{si} \rightarrow 0 \text{ and } t_c = t_i \exp \left[\frac{8\lambda_c}{3\pi^2} \left(\frac{s_{ce}}{t_i} \right)^2 \right] \text{ for } \lambda_{si} \rightarrow \infty. \quad (58)$$

The variation of the physical free fall time t_c with λ_{si} is also presented in Fig. 6 if correction factor $\lambda_c = 1$ (the right axis). Conversely, Eq. (57) can be used to estimate the start time t_i of a free fall if the free fall time t_c is known.

The free fall time t_c increases if the same two-body system starts to collapse at an earlier time t_i . This is expected because the Hubble constant (damping) is greater at earlier time where larger resistance to the gravitational collapse is expected. Time t_c approaches s_{ce} when s_{ce} is small (small separation or large mass) or when initial time t_i approaches t_0 . Clearly, larger λ_{si} (either greater separation between two body $r_i \rightarrow \infty$ or smaller total mass $M \rightarrow 0$ in Eq. (44)) or smaller t_i (free fall starts at earlier physical time) will lead to a much larger free fall time than the exact free fall time in static background ($t_c \gg s_{ce}$).

3.4 TBCM model in the simplest form and perturbative solutions for equilibrium collapse

Next, the equation for $F(s)$ can be further simplified by introducing an amplitude function $F_a(\omega_m s)$. The original frequency function $F(s)$ can be decoupled into the product of the mean solution $F_m(s)$ (Eq. (39)) and an amplitude function $F_a(\omega_m s)$ as

$$F(s) = F_m(s) F_a(\omega_m s) = \gamma_s^{-1/(2+n)} \left(\frac{r_i}{v_i} \right)^{1/2} \exp\left(-\frac{2-n}{2+n} \cdot \frac{H_0 s}{4} \right) F_a(\omega_m s). \quad (59)$$

Substitution of Eq. (59) into the original Eq. (34) for $F(s)$ leads to a very simple equation for the amplitude function $F_a(x)$ with respect to a dimensionless variable $x = \omega_m(s)s$,

$$\frac{\partial^2 F_a(x)}{\partial x^2} = \underbrace{\frac{2n}{(2-n)^2} \frac{F_a(x)}{x^2}}_1 - \underbrace{F_a^{n-1}(x)}_2 + \underbrace{F_a^{-3}(x)}_3, \quad (60)$$

with initial conditions (using Eq. (35)),

$$F_a(x_0) = \gamma_s^{1/(2+n)} \quad \text{and} \quad \left. \frac{\partial F_a}{\partial x} \right|_{x=x_0} = \frac{\beta_s \gamma_s^{-1/(2+n)}}{2+n} \quad \text{with} \quad x_0 = \frac{2\gamma_s^{2/(2+n)}}{\beta_s} \frac{2+n}{2-n}, \quad (61)$$

where the ratio $\gamma_s = (v_{ri}/v_i)^2$ with v_{ri} from Eq. (22), v_i is the initial speed and the parameter $\beta_s = 4\lambda_s = H_0 r_i / v_i$ is introduced for convenience. Similarly, parameter $\beta_{si} = 4\lambda_{si} = H_0 r_i / v_{ri}$ can be defined (Eq. (44)). Note that Eq. (60) is exact and is the simplest representation of original problem (Eqs. (11)). Solution is fully determined by three dimensionless parameters, i.e. n , β_s and γ_s , a significant reduction from five parameters in original Eq. (30).

For small x or $n = -2$, term 1 (damping force) on the RHS of Eq. (60) is dominant and we have the exact solution of

$$F_a(x \rightarrow x_0) = \left(\frac{\beta_s \gamma_s^{-1/2}}{2} \frac{2-n}{2+n} x \right)^{2/(2-n)}, \quad (62)$$

which is consistent with the transient solution in Eq. (36).

For large x , term 2 (gravitational force) and term 3 (frequency force due to the angular momentum) are dominant. The trivial solution $F_a(x) = 1$ can be easily identified for $\gamma_s = 1$ and $\beta_s = 0$ (i.e. static background without damping). If $n = -1$ and $\beta_s = 0$, the original problem is reduced to the classical two-body gravitational problem in static background without damping.

Here we focus on a more general case with a weak damping $\beta_s \rightarrow 0$ and $-2 < n < 0$ (large $x \geq x_0 \gg 0$ from Eq. (61)), where the competition between terms 2 and 3 leads to an oscillatory solution vibrating around the mean value $F_a(x) = 1$. It can be easily shown that if $F_a(x) < 1$, we

have $F_a^{-3}(x) > F_a^{n-1}(x)$, the positive curvature $\partial^2 F_a(x)/\partial x^2 > 0$ from Eq. (60) brings $F_a(x)$ back to $F_a(x) > 1$; If $F_a(x) > 1$, we have $F_a^{-3}(x) < F_a^{n-1}(x)$, curvature $\partial^2 F_a(x)/\partial x^2 < 0$ brings $F_a(x)$ back to the region $F_a(x) < 1$; No oscillatory solution exists for short range force with $n \leq -2$.

We are especially interested in the oscillatory solutions with a weak damping ($\beta_s \rightarrow 0$), which is more relevant to the gravitational collapse in large-scale N -body simulations. For weak damping, a harmonic function can be used to approximate the solution of Eq. (60),

$$F_a(x) \approx A_0 + A_1 \sin[k_s(x - x_0) + A_3], \quad (63)$$

where A_0 is the mean value, A_1 is the amplitude, A_3 is the phase angle, and k_s is a dimensionless frequency. Substitution of Eq. (63) into Eq. (60), the frequency k_s can be approximated by,

$$k_s \approx \left| (n-1)A_0^{n-2} + 3A_0^{-4} \right|^{1/2}. \quad (64)$$

To satisfy the boundary conditions (Eq. (61)), we have

$$A_0 + A_1 \sin(A_3) = \gamma_s^{1/(2+n)} \quad \text{and} \quad k_s A_1 \cos(A_3) = \frac{\beta_s \gamma_s^{-1/(2+n)}}{(2+n)}. \quad (65)$$

Two limiting situations can be identified for the case of weak damping ($\lambda_s \rightarrow 0$):

- 1) Small initial velocity v_i where $\gamma_s = (v_{ri}/v_i)^2 \gg 1$. This is the free fall collapse and free fall time is discussed in Section 3.3.
- 2) Large initial velocity v_i where $\gamma_s = (v_{ri}/v_i)^2 \ll 1$. There exists a point in the trajectory with a vanishing kinetic energy and maximum potential (turning point). If this point is considered as the initial position, the trajectory after this point should be a free fall that is considered in 1). Therefore, both 1) and 2) will not likely lead to oscillatory motion.

3) A more interesting case is the special case we discussed before, namely the initial velocity $v_i \approx v_{ri}$ and $\gamma_s = (v_{ri}/v_i)^2 \approx 1$ for initial system close to virial equilibrium. This case leads to an equilibrium collapse with oscillatory solutions, as shown in Fig. 5. For this case, $A_0 = 1 \gg A_1$ (the fluctuation is small compared to the mean solution in Eq. (63)), $k_s = \sqrt{2+n}$ (from Eq. (64)), and $A_3 = 0$. Final perturbative solution for the amplitude function $F_a(x)$ (first order of β_s) reads

$$F_a(x) \approx 1 + \frac{\beta_s}{(2+n)^{3/2}} \sin\left[\sqrt{2+n}(x-x_0)\right] = 1 + \frac{\beta_s}{(2+n)^{3/2}} \sin(\theta_s(x)), \quad (66)$$

where the angle function θ_s is (with Eq. (41) for ω_m and Eq. (40) for mean radius r_m)

$$\theta_s(x) \equiv \theta_s(\omega_m s) = \sqrt{2+n}(\omega_m s - x_0) = \frac{2\sqrt{2+n}}{\beta_s} \frac{2+n}{2-n} \left[\left(\frac{r_m}{r_i} \right)^{-(2-n)/2} - 1 \right], \quad (67)$$

Or equivalently

$$\theta_s(s) = \frac{2\sqrt{2+n}}{\beta_s} \frac{2+n}{2-n} \left[\exp\left(\frac{2-n}{2+n} \cdot \frac{H_0 s}{2}\right) - 1 \right] \approx \sqrt{2+n} \frac{sv_i}{r_i} \text{ for } H_0 s \ll 1, \quad (68)$$

which approximates the angle swept by the displacement vector \mathbf{r} within time s if $H_0 s \ll 1$.

Obviously solution (66) is valid only for $\beta_s < (2+n)^{3/2}$ such that the amplitude of oscillation is less than one in Eq. (66) for a positive amplitude function $F_a(x)$.

Solutions for $\beta_s = 0$ and $n = -1$ are well known for two-body gravitational problem in static background. Table 1 presents a summary for different competitions between gravity, damping, and angular momentum for $\beta_s \neq 0$ and $-2 < n < 0$.

Table 1. Competition among gravity, damping and angular momentum for $\beta_s \neq 0$ and $n = -1$.

	$\beta_s = H_0 r_i / v_i \ll 1$	$\beta_s = H_0 r_i / v_i \sim 1$	$\beta_s = H_0 r_i / v_i \gg 1$
$\gamma_s \ll 1$	$H_0 r_i \ll v_{ri} \ll v_i (\beta_{si} \ll 1)$ $v_{ri} \ll H_0 r_i \ll v_i (\beta_{si} \gg 1)$ $H_0 r_i \approx v_{ri} \ll v_i (\beta_{si} \approx 1)$	$v_{ri} \ll H_0 r_i \approx v_i (\beta_{si} \gg 1)$	$v_{ri} \ll v_i \ll H_0 r_i (\beta_{si} \gg 1)$
$\gamma_s \sim 1$	$H_0 r_i \ll v_{ri} \approx v_i (\beta_{si} \ll 1)$ Equilibrium collapse	$v_{ri} \approx H_0 r_i \approx v_i (\beta_{si} \approx 1)$	$v_{ri} \approx v_i \ll H_0 r_i (\beta_{si} \gg 1)$
$\gamma_s \gg 1$	$H_0 r_i \ll v_i \ll v_{ri} (\beta_{si} \ll 1)$ Free collapse	$v_i \approx H_0 r_i \ll v_{ri} (\beta_{si} \ll 1)$ Free collapse	$v_i \ll H_0 r_i \approx v_{ri} (\beta_{si} \approx 1)$ $v_i \ll v_{ri} \ll H_0 r_i (\beta_{si} \gg 1)$ $v_i \ll H_0 r_i \ll v_{ri} (\beta_{si} \ll 1)$ Free collapse

For a fixed mean radius $r_m(s)$, two-body systems with different initial separation r_i can have different angle θ_s that is dependent on r_i (Eq. (67)). Other relevant solutions can be found as,

$$F(s) = F_m(s) F_a(\omega(s)s) = \left(\frac{r_i}{v_i}\right)^{1/2} \exp\left(-\frac{2-n}{2+n} \cdot \frac{H_0 s}{4}\right) \left\{1 + \frac{\beta_s}{(2+n)^{3/2}} \sin(\theta_s)\right\}, \quad (69)$$

$$r(s) = r_m(s) F_a(\omega_m(s)s) = r_i \exp\left(-\frac{H_0 s}{2+n}\right) \left\{1 + \frac{\beta_s}{(2+n)^{3/2}} \sin(\theta_s)\right\}, \quad (70)$$

the frequency function $\omega(s)$ from Eq. (28)

$$\omega(s) = \frac{1}{s} \int F_m^{-2}(s) F_a^{-2}(\omega_m(s)s) ds, \quad (71)$$

and the time derivative of radius (or the radial velocity)

$$\dot{r} = \frac{\partial r(s)}{\partial s} = \frac{H_0 r_i}{(2+n)} \exp\left(-\frac{n H_0 s}{2(2+n)}\right) \cos(\theta_s) - \frac{H_0 r}{2+n}. \quad (72)$$

Note that the first term on the RHS (right hand side) of Eq. (72) is from the time variation of angle θ_s . This term becomes dominant over the second term with $r \rightarrow 0$ but can be averaged out for random θ_s . This expression will be used for deriving the stable clustering hypothesis (SCH) in

Section 4.1 (Eq. (114)). For a given potential exponent n , parameter β_s controls both amplitude and period of vibration (Eqs. (68) and (69)).

The temporal evolution in transformed system with time scale s can be equivalently transformed back to the evolution in original comoving system with physical time t (Eq. (53)), where $s = t_0 \ln(t/t_i)$. Here t_i (or a_i) is the initial time (or initial scale factor) and t_0 is the physical time of the present epoch. The exponential evolution with time s is equivalent to a power-law evolution with the physical time t ,

$$\exp(\tau H_0 s) \rightarrow (a/a_i)^\tau. \quad (73)$$

After transforming back to the comoving system, the mean separation r_m

$$r_m \propto \exp(-H_0 s / (2+n)) = (a/a_i)^{-1/(2+n)} \quad (74)$$

can be obtained from Eq. (40) for the equilibrium range in Fig. 5. Stable clustering hypothesis (SCH) refers to a comoving separation $r_m \propto a^{-1}$ or a fixed proper separation frozen in the physical time t . Clearly, only the equilibrium collapse with $n = -1$ will lead to the stable clustering in expanding background (Eq. (74)).

3.5 Critical values of β_s for equilibrium collapse and critical density

For convenience, numerical constant $\beta_s = 4\lambda_s = H_0 r_i / v_i$ is introduced to quantify the competition between expanding background and gravity. Two critical values of β_s can be identified from TBCM model and its solutions. Let's consider a two-body system that starts to collapse at an initial physical time t_i with a corresponding Hubble constant H_i and scale factor

a_i . The evolution of angle function θ_s and separation r in time scale s (Eqs. (68) and (70)) can be equivalently transformed back to the evolution in physical time t , where

$$\theta_s(t) = \frac{1}{2\lambda_s} \frac{(2+n)^{3/2}}{2-n} \left[\exp\left(\frac{2-n}{2+n} \cdot \frac{H_0 s}{2}\right) - 1 \right] = \frac{2}{\beta_s} \frac{(2+n)^{3/2}}{2-n} \left(\left(\frac{t}{t_i}\right)^{\frac{2-n}{3(2+n)}} - 1 \right), \quad (75)$$

$$r(t) = r_i \left(\frac{a_i}{a}\right)^{1/(2+n)} \left\{ 1 + \frac{\beta_s}{(2+n)^{3/2}} \sin[\theta_s(t)] \right\}. \quad (76)$$

Specifically, for $n = -1$,

$$r(t) = r_i \left(\frac{a_i}{a}\right) \left\{ 1 + \beta_s \sin \left[\frac{2}{3\beta_s} \left(\frac{t}{t_i} - 1 \right) \right] \right\} \quad \text{and} \quad \theta_s(t) = \frac{2}{3\beta_s} \left(\frac{t}{t_i} - 1 \right). \quad (77)$$

The first critical value of β_s can be easily identified for the existence of an equilibrium range from Eq. (76), i.e.

$$\beta_{s1} = \frac{H_0 r_{ic}}{v_{ic}} = (2+n)^{3/2}, \quad (78)$$

which leads to a critical initial separation r_{ic} or initial velocity v_{ic} when combined with Eq. (22),

$$r_{ic} = \frac{1}{2} \left[\frac{-nG_n(m_1 + m_2)}{H_0^2 (2+n)^{-3}} \right]^{1/(2-n)} \quad \text{and} \quad v_{ic} = \frac{1}{2} \frac{[-nG_n(m_1 + m_2)]^{1/(2-n)}}{[H_0 (2+n)^{-3/2}]^{n/(2-n)}}. \quad (79)$$

Both r_{ic} and v_{ic} are only dependent on the system mass, the damping H_0 and the potential exponent n . For $m_1 = m_2 = 2.27 \times 10^{11} M_{sun}/h$, $r_{ic} = 0.29 \text{ Mpc}/h$ and $v_{ic} = 29 \text{ km}/s$. This is the maximum separation and the corresponding velocity for the existence of an equilibrium two-body collapse.

For systems that evolve from initial virial equilibrium (the special case $\gamma_s = (v_{ri}/v_i)^2 = 1$), the equilibrium collapse exists only if $\beta_s \leq \beta_{s1} = (2+n)^{3/2}$ (or $r_i < r_{ic}$ or $v_i = v_{ri} > v_{ic}$), where gravity is sufficiently large to balance expanding background in order to form the equilibrium collapse. For $\beta_s > \beta_{s1} = (2+n)^{3/2}$, gravity is too weak to establish an equilibrium collapse.

Next, let us consider a continuous growth of a large halo starting from $t = 0$ to $t = t_0$ with an infinitesimal lifetime and extremely fast mass accretion. This halo is formed by continuously growing via a sequence of two-body collapse (merging) events with single mergers with an infinitesimal waiting time. Therefore, halos grow with an infinitesimal lifetime is an extreme case and should always have a vanishing

$$\sin[\theta_s(t)] = 0 \text{ for any } t \in [0, t_0], \quad (80)$$

such that $r(t) = r_m$ in Eqs. (70) and (76) from $t = 0$ to $t = t_0$ without oscillation. Let us assume the first merging event occurs at time t_i . With $t_i \rightarrow 0$, we can safely assume that $k = t/t_i$ is an integer. From Eqs. (75) and (80),

$$\sin[\theta_s(t)] = \sin\left[\frac{2}{\beta_s} \frac{(2+n)^{3/2}}{2-n} \left(k^{\frac{2-n}{3(2+n)}} - 1\right)\right] = 0. \quad (81)$$

The second critical value of β_s can be identified from Eq. (81) for any arbitrary integer k ,

$$\beta_{s2} = \frac{(2+n)^{3/2}}{(2-n)\pi}. \quad (82)$$

Note that there exists a constant value of β_{s2} satisfying Eq. (81) for any integer k if and only if

$$n = \frac{2-6m}{1+3m} \text{ with integer } m = 1, 2, \dots, \infty \text{ and } \beta_{s2} = \frac{2}{3\pi m \sqrt{1+3m}} \quad (83)$$

for a discrete sequence of gravity exponent $n = -1, -10/7, -8/5, \dots, -2$. Specifically, $\beta_{s_2} = 1/(3\pi)$ for $n = -1$ and $\beta_{s_2} = 1/(3\pi\sqrt{7})$ for $n = -10/7$. The parameter β_s for large halos with infinitesimal waiting time should always satisfy $\beta_s = \beta_{s_2}$. The time derivative of the angle θ_s (angular speed) can be easily obtained from Eq. (75),

$$\left. \frac{d\theta_s}{dt} \right|_{t=t_i} = \frac{2\sqrt{2+n}}{3\beta_{s_2}t} = \frac{(2-n)}{(2+n)} \frac{2\pi}{3t}, \quad (84)$$

from which we can find the period T_s for large halos formed at any instant time t ,

$$T_s = \frac{2\pi}{d\theta_s/dt} = \frac{3(2+n)}{(2-n)} t = \frac{t}{m}. \quad (85)$$

Specifically, for large halos with an infinitesimal lifetime and $n = -1$, halos formed at any instant t from a two-body collapse with a single merger has a period of $T_s = t$ (the orbital period of outer region of halos should be comparable to the current physical time t).

Two numerical constants α_s (in Eq. (24)) and $\beta_s = H_0 r_i / v_i$ are closely related to the density ratio of two-body system to the background. Let's consider large halos start equilibrium collapse at physical time t_i with a corresponding Hubble constant H_i ($H_0^2 = H_i^2 a_i^3$) and scale factor a_i .

The two numerical constants are defined as

$$\beta_s = \frac{H_0 r_i}{v_i} = \frac{H_0 r_i}{u_i a_i^{1/2}} = \frac{H_i r_{yi}}{u_i}, \quad \alpha_s = \frac{v_i^2 r_i^{-n}}{G_n m_h} = \frac{u_i^2 a_i r_i^{-n}}{G_n m_h} = \frac{u_i^2 r_{yi}^{-n} a_i^{n+1}}{G_n m_h}. \quad (86)$$

Here α_s is the virial constant from Eq. (24), $u_i = v_i a_i^{-1/2}$ is the peculiar velocity at time t_i , v_i is the velocity in transformed system with time scale s , and $r_{yi} = a_i r_i$ is the separation in physical coordinate at time t_i . Large halos with infinitesimal lifetime are synchronized. All halos are generated at the same time t and both constants α_s and β_s should approach constant values (Eqs.

(82) and (24)), i.e a direct delta distribution. For small halos with a finite lifetime, there can be a distribution of values of α_s and β_s since small halos are generated at different initial time t_i can co-exist at the same time t .

Note that $H^2 = 8\pi G\bar{\rho}_y(t)/3$, where $\bar{\rho}_y(t)$ is the physical density of background, Eq. (86) can be used to derive a ratio Δ of the physical density of halos to the background density at time t_i ,

$$\Delta = \frac{\rho_s(t_i)}{a_i^3 \bar{\rho}_y(t_i)} = \frac{\rho_y(t_i)}{\bar{\rho}_y(t_i)} = \frac{1}{4\alpha_s \beta_s^2} \frac{G}{G_n r_i^{1+n}}. \quad (87)$$

Here ρ_y is the mean physical density of halo. Comoving density ρ_s of the two-body system is

$$\rho_s(t_i) = \frac{M}{4\pi(2r_i)^3/3}, \quad (88)$$

where $M = m_1 + m_2$ and the halo size is $r_h = 2r_i$ because of $m_1 \ll m_2$ (large halo merges with a single merger where the mass of a single merger is much smaller) and $\mu = 2$ (in Eq. (12)).

The critical density can be computed based on two critical values β_{s1} and β_{s2} . For gravitational collapse of a two-body system with $n = -1$, $G = G_n$, $\alpha_s = -n/2^{2-n} = 1/8$ (Eq. (24)), and $\beta_s < \beta_{s1} = 1$, only the system with a physical density $\rho_y(t_i) > 2\bar{\rho}_y(t_i)$ (from Eq. (87)) will lead to an equilibrium collapse. Systems with a physical density $\rho_y(t_i) < 2\bar{\rho}_y(t_i)$ will have a free fall collapse that can be completed in a much short period (Fig. 5).

For $n = -1$, the density ratio Δ of large halos with an infinitesimal lifetime and $\beta_s = \beta_{s2}$ is (from Eqs. (87), (82), and $\alpha_s = -n/2^{2-n}$),

$$\Delta = \frac{\rho_y(t_i)}{\bar{\rho}_y(t_i)} = \frac{1}{4\alpha_s \beta_{s2}^2} = -\frac{2^{-n}(2-n)^2}{n(2+n)^3} \pi^2 = 18\pi^2 \text{ for } n = -1. \quad (89)$$

Surprisingly, this critical density ratio is consistent with the prediction from spherical collapse model (SCM) and reveals deep connections between TBCM and SCM models. More discussion will be presented in Sections 4.3.

3.6 Solutions for energy, virial quantity, and angular momentum

We can demonstrate that the specific kinetic and potential energies (per unit mass) for two-body collapsing system are evolving exponentially in the time scale s (or equivalently a power-law with respect to a in the original comoving system using Eq. (73)). The specific kinetic energy reads (from Eqs. (17), (18), and (28))

$$K_s = \frac{1}{(m_1 + m_2)} \left[\frac{1}{2} m_1 (v_{x1}^2 + v_{y1}^2) + \frac{1}{2} m_2 (v_{x2}^2 + v_{y2}^2) \right] = \frac{2m_1 m_2}{(m_1 + m_2)^2} \left[\underbrace{\dot{r}_1^2}_1 + \underbrace{r^2 F(s)^{-4}}_2 \right]. \quad (90)$$

The first term (term1) on the RHS represents the contribution from the radial motion that is small when compared to the second term. The ratio between two terms on the RHS of Eq. (90) can be obtained from Eqs. (32) and (69),

$$\left[\frac{\dot{r}}{rF(s)^{-2}} \right]^2 = F^4 \left(\frac{\partial \ln F}{\partial s} - \frac{H_0}{4} \right)^2 \approx \frac{\beta_s^2}{(2+n)^2} \exp\left(-\frac{2-n}{2+n} \cdot H_0 s \right). \quad (91)$$

For small β_s , this ratio is exponentially decaying with time s and proportional to β_s^2 (second order). By neglecting the high order term (term 1) and using Eqs. (69) for $F(s)$ and Eq. (70) for $r(s)$, the final expression of the specific kinetic energy reads

$$K_s \approx \frac{2m_1 m_2 v_i^2}{(m_1 + m_2)^2} \exp\left(\frac{-nH_0 s}{2+n} \right) \left[1 - \frac{2\beta_s}{(2+n)^{3/2}} \sin \theta_s \right]. \quad (92)$$

Similarly, the specific potential energy reads (with the expression of r from Eq. (70) and v_i^2

from Eq. (24)),

$$P_s = -\frac{G_n m_1 m_2}{(2r)^{-n}} \frac{1}{(m_1 + m_2)} \approx \frac{2m_1 m_2 v_i^2}{(m_1 + m_2)^2} \exp\left(\frac{-nH_0 s}{2+n}\right) \left[\frac{2}{n} + \frac{2\beta_s}{(2+n)^{3/2}} \sin \theta_s \right]. \quad (93)$$

The total energy of two-body system and that of each individual mass are

$$E_s = K_s + P_s = \frac{(2+4/n)m_1 m_2 v_i^2}{(m_1 + m_2)^2} \exp\left(\frac{-nH_0 s}{2+n}\right) = \frac{-(2+n)m_1 m_2}{(m_1 + m_2)} \frac{G_n r_i}{(2r_i)^{1-n}} \exp\left(\frac{-nH_0 s}{2+n}\right), \quad (94)$$

$$E_{s1} = \left(\underbrace{\frac{-nm_2^2}{m_1 + m_2}}_{\text{kinetic}} \underbrace{-m_2}_{\text{potential}} \right) \frac{(-2)v_i^2}{n(m_1 + m_2)} \exp\left(\frac{-nH_0 s}{2+n}\right) = \left(\underbrace{\frac{-nm_2^2}{m_1 + m_2}}_{\text{kinetic}} \underbrace{-m_2}_{\text{potential}} \right) \frac{G_n r_i}{(2r_i)^{1-n}} \exp\left(\frac{-nH_0 s}{2+n}\right), \quad (95)$$

$$E_{s2} = \left(\frac{-nm_1^2}{m_1 + m_2} - m_1 \right) \frac{(-2)v_i^2}{n(m_1 + m_2)} \exp\left(\frac{-nH_0 s}{2+n}\right) = \left(\frac{-nm_1^2}{m_1 + m_2} - m_1 \right) \frac{G_n r_i}{(2r_i)^{1-n}} \exp\left(\frac{-nH_0 s}{2+n}\right), \quad (96)$$

respectively. As shown in Fig. 3, both K_s and P_s vibrate about their mean solutions with an amplitude proportional to the parameter β_s to the first order. The specific energy E_s does not vibrate due to the cancellation of first order perturbation in K_s and P_s (Eq. (94)).

By considering an ensemble of many two-body systems with randomly distributed angles θ_s , the ensemble average of kinetic and potential energies of these two-body systems are

$$\langle K_s \rangle = \frac{2m_1 m_2 v_i^2}{(m_1 + m_2)^2} \exp\left(\frac{-nH_0 s}{2+n}\right)$$

and

$$\langle P_s \rangle = \frac{4m_1 m_2 v_i^2}{n(m_1 + m_2)^2} \exp\left(\frac{-nH_0 s}{2+n}\right), \quad (97)$$

where first order perturbations are averaged out. The average kinetic and potential energy satisfy the virial equilibrium where $2\langle K_s \rangle - n\langle P_s \rangle = 0$ in the equilibrium range.

The system spends most time in the equilibrium range with an exponential evolution of energy in time scale s (from Eqs. (92), (93) and (97)). Equivalently, energy follows a power-law evolution in physical time t , i.e. $\langle K_s \rangle \propto t$ and $\langle P_s \rangle \propto t$ for $n=-1$, that will provide some clues for the energy evolution in large scale N-body system (discussed in a separate paper).

More interestingly for $n=-1$, the evolution of specific energy of two individual particles (Eqs. (95) and (96)) is the same for both particles regardless of their masses, where $E_s = E_{s1} = E_{s2}$. For a two-body system with unequal mass $m_1 \neq m_2$, the specific energy is independent of particle mass ($E_{s1} = E_{s2}$), while the total energy is proportional to particle mass. The energy equipartition does not apply for the two-body system in equilibrium range, where there is no energy transfer between two particles. The energy evolution does not depend on individual mass, which seems consistent with the concept of violent relaxation. More discussion is presented in Section 4.2.

The temporal evolution of the specific virial quantity G_s (mass averaged radial velocity moment) can be found from Eqs. (13) and (14), where G_s is defined as,

$$G_s = \frac{\sum m_i \mathbf{x}_i \cdot \mathbf{v}_i}{\sum m_i} = \frac{m_1 \mathbf{x}_1 \cdot \mathbf{v}_1 + m_2 \mathbf{x}_2 \cdot \mathbf{v}_2}{m_1 + m_2} = \frac{4m_1 m_2}{(m_1 + m_2)^2} \mathbf{r} \cdot \mathbf{v} = \frac{4m_1 m_2}{(m_1 + m_2)^2} \dot{r} r. \quad (98)$$

Using Eqs. (70) and (72) for radius r and \dot{r} , the specific virial quantity G_s can be written as,

$$G_s = \frac{4m_1 m_2}{(m_1 + m_2)^2} \left\{ \frac{H_0 r_i^2}{(2+n)} \exp\left(-\frac{H_0 s}{2}\right) \left(\cos \theta_s + \frac{\beta_s}{2(2+n)^{3/2}} \sin 2\theta_s \right) - \frac{H_0 r_i^2}{2+n} \exp\left(-\frac{2H_0 s}{2+n}\right) \left(1 + \frac{\beta_s}{(2+n)^{3/2}} \sin \theta_s \right)^2 \right\}. \quad (99)$$

Similarly, the specific angular momentum of the two-body system can be obtained as,

$$\begin{aligned}\mathbf{H}_s &= \frac{m_1 \mathbf{x}_1 \times \mathbf{v}_1 + m_2 \mathbf{x}_2 \times \mathbf{v}_2}{m_1 + m_2} = \frac{4m_1 m_2}{(m_1 + m_2)^2} \mathbf{r} \times \mathbf{v} \\ &= \frac{4m_1 m_2}{(m_1 + m_2)^2} r^2 F^{-2}(s) \hat{\mathbf{z}} = \frac{4m_1 m_2 v_i r_i}{(m_1 + m_2)^2} \exp\left(-\frac{1}{2} H_0 s\right) \hat{\mathbf{z}}.\end{aligned}\quad (100)$$

The angular momentum \mathbf{H}_s decays exponentially at a rate of $H_0/2$ that is independent of the potential exponent n .

3.7 The two-body angular velocity ω_t , critical angle θ_{vr} , and halo kinetic energy

The two-body collapse model (TBCM) and its solutions are presented. The two critical density ratios are identified. Rich information contained in TBCM model can be used to provide more insights into the structure formation and energy evolution. This section presents several applications of TBCM besides the critical density ratio.

The first example is about the two-body angular velocity ω_s that can be found from the kinetic energy solution with

$$\frac{1}{2} \left(m_1 \mu^2 + m_2 (2 - \mu)^2 \right) \omega_s^2 r^2 = (m_1 + m_2) K_s. \quad (101)$$

With r from Eq. (70), $\mu = 2m_2/(m_1 + m_2)$ from Eq. (12), and kinetic energy from Eq. (92), the angular velocity ω_s in transformed system is obtained from Eq. (101),

$$\omega_s \approx \frac{v_i}{r_i} \exp\left[\frac{2-n}{2(2+n)} H_0 s \right]. \quad (102)$$

For $n = -1$, angular velocity ω_t in original comoving system (with $\gamma_s = 1$ and r_m in Eq. (40) and Eq. (73) for transformation) is,

$$\omega_i = \omega_s \frac{ds}{dt} = \omega_s a^{-3/2} = \frac{r_i^{3/2}}{\beta_s} H r_m^{-3/2}, \quad (103)$$

where the two-body angular velocity $\omega_i \sim H r_m^{-3/2}$ is inversely proportional to the mean separation r_m and is proportional to the Hubble constant.

The second example is about the angle θ_{vr} between particle velocity and the vector of separation. The virial quantity G_s (Eqs. (98) and (99)) represents the relative motion of two particles in the radial direction, while \mathbf{H}_s (Eq. (100)) stands for the relative motion in the tangential direction. Terms involving θ_s in Eq. (99) can be averaged out when averaging over many two-body systems with random angle θ_s . The angle θ_{vr} between the displacement vector \mathbf{r} and its velocity vector \mathbf{v} can be computed using Eqs. (99), (100), Eq. (70) for r , and the transformation between time scales $s = t_0 \ln(t/t_i)$,

$$\cot(\theta_{vr}) = -\frac{v_r}{v_{cir}} = \frac{\mathbf{r} \cdot \mathbf{v}}{|\mathbf{r} \times \mathbf{v}|} = \frac{G_s}{|\mathbf{H}_s|} \approx -\frac{H_0 r_i}{v_i (2+n)} \exp\left(\frac{n-2}{2(n+2)} H_0 s\right) = -\frac{\beta_s}{(2+n)} \left(\frac{a}{a_i}\right)^{\frac{n-2}{2(n+2)}}, \quad (104)$$

where v_r is the radial velocity and v_{cir} is the circular velocity. For $\beta_s = \beta_{s2}$, i.e. halos with an infinitesimal lifetime, the angle θ_{vr} is slightly $> \pi/2$ (i.e. $\cot(\theta_{vr}) \approx \cos(\theta_{vr})$) due to the gravitational interaction. Equation (104) predicts that for two-body system, the angle θ_{vr} between the pairwise velocity $\Delta \mathbf{u} = \mathbf{u}_1 - \mathbf{u}_2$ and their separation vector $\Delta \mathbf{r} = \mathbf{r}_1 - \mathbf{r}_2$ satisfies

$$\cot(\theta_{vr}) = -\beta_s \left(\frac{a}{a_i}\right)^{-3/2} = -\beta_s \left(\frac{r_m}{r_i}\right)^{3/2}, \quad (105)$$

where r_m is the mean separation and $\theta_{vr} \rightarrow \pi/2$ with time t or a . For two-body collapse between large halos with an infinitesimal lifetime and a single merger, $\beta_s = \beta_{s2}$ and $\cot(\theta_{vr}) = -1/(3\pi)$

such that the angle between the velocity \mathbf{v} of that single merger at halo surface and its position vector \mathbf{r} from halo center should be $\theta_{vr} \approx 96.06^\circ$, which is consistent with the result in [14] (Eq. (31)) for halos with an isothermal density profile. The ratio of the radial velocity of single merger to its circular velocity is always a constant $v_r/v_{cir} = \beta_{s2} = 1/3\pi$. Halo with an isothermal density profile seems to be a direct result of infinitesimal waiting time that also can be demonstrated by the application of TBCM model to derive halo energy.

The last example is to derive the kinetic and potential energy for large halos with an infinitesimal lifetime. Let's consider a halo of mass M with a specific peculiar kinetic energy K_h that is continuously growing via elementary two-body merging with a single merger of mass dM during an infinitesimal time dt . Since $dt \approx 0$, the change of total kinetic energy of two-body system in transformed system will be $(M + dM) \cdot K_s(s=0)$ with K_s from Eq. (92). The incremental change of the specific peculiar kinetic energy in comoving system from a single merging event is

$$dK_h = \frac{K_s(s=0)}{a} = \frac{2M}{M^2} dM \frac{v_i^2}{a} = \frac{2M}{M^2} dM \cdot \alpha_s \frac{G_n M}{a r_i^{-n}}, \quad (106)$$

where the last equality is from the fact that $v_i^2 = \alpha_s G_n M / r_i^{-n}$ (Eq. (24)) and r_i is the comoving length of the displacement vector. Since $dt \approx 0$, the merging is instantaneous. The halo mass $M \propto r_i^3$ and the halo kinetic energy $K_h \propto G_n M / r_i^{-n} \propto M^{1+n/3}$ for halos of different mass at the same redshift (virial theorem). Therefore, from Eq. (106)

$$\frac{d \ln K_h}{d \ln M} = \frac{2\alpha_s G_n M}{K_h a r_i^{-n}} = 1 + \frac{n}{3}. \quad (107)$$

The final expressions for halo kinetic and potential energy are: (using the virial theorem for halos $2K_h - n_e P_h = 0$, where $n_e \approx -1.3$ is an effective exponent considering the mass cascade and halo surface energy and $n_e \approx -1.5$ for halos with an isothermal density (Eq. (96) in [14]))

$$K_h = \frac{6\alpha_s}{3+n} \frac{G_n M}{ar_i^{-n}} \quad \text{and} \quad P_h = \frac{12}{(3+n)} \frac{\alpha_s}{n_e} \frac{G_n M}{ar_i^{-n}}. \quad (108)$$

The one-dimensional velocity dispersion

$$\sigma_v^2 = \frac{2}{3} K_h = \frac{4\alpha_s}{3+n} \frac{G_n M}{ar_i^{-n}}, \quad (109)$$

with $\alpha_s = -n/2^{2-n}$ defined in Eq. (24). Specifically, for $n = -1$,

$$K_h = \frac{3}{8} \frac{GM}{ar_i} = \frac{3}{8} \frac{GM}{r_{yi}} = \frac{3}{4} \frac{GM}{r_h}, \quad P_h = \frac{3}{4} \frac{GM}{n_e ar_i} = \frac{3}{2n_e} \frac{GM}{r_h}, \quad (110)$$

and halo virial dispersion

$$\sigma_v^2 = \frac{2}{3} K_h = 2 \frac{v_i^2}{a} = 2u_i^2 = \frac{1}{4} \frac{GM}{ar_i} = \frac{GM}{2r_h}, \quad (111)$$

where $r_{yi} = ar_i = r_h/2$ is the length of displacement vector in physical coordinate and r_h is halo size. For large halos merging with a single merger such that $m_2 \gg m_1$, $\mu = 2$, and $r_{yi} = r_h/2$ (from Eqs. (12) and (15)). Here $v_i^2 = GM/8r_i$ (Eq. (24)). Surprisingly, the halo kinetic and potential energies can be derived simply based on the elementary two-body collapse for large halos with an infinitesimal lifetime, where halo density profile information is not even required.

On the other hand, the halo potential energy can be obtained for halos with a power-law density profile of $\rho_h(r) \sim r^{-m}$,

$$P_h = -\frac{\int_0^{r_h} \frac{G}{y} \left[\int_0^y \rho_h(x) 4\pi x^2 dx \right] \rho_h(y) 4\pi y^2 dy}{\int_0^{r_h} \rho_h(x) 4\pi x^2 dx} = -\frac{3-m}{5-2m} \frac{GM}{r_h}. \quad (112)$$

The potential energy from an isothermal profile with $m=2$ (Eq. (112)) is exactly consistent with that from the TBCM model in Eq. (110) (the effective potential exponent $n_e = -1.5$ for isothermal density (Eq. (96) in [14])). This fact indicates that the isothermal density profile of large halos is a direct result of extremely fast mass accretion or infinitesimal lifetime. In reality, halos have finite lifetime, and the density profile cannot be exactly isothermal.

4. Connections with existing theories

Solutions developed for TBCM model in Section 3 provide significant insights into existing theories. In this Section, TBCM model is applied to demonstrate the stable clustering hypothesis (SCH). The generalized stable clustering hypothesis (GSCH) is proposed with an interesting scaling for high order moments of pairwise velocity. Finally, the connections with violent relaxation and standard spherical collapse model (SCM) are also discussed.

4.1 Connections with stable clustering hypothesis (SCH) and generalized SCH

The stable clustering hypothesis is a fundamental assumption and one of the few key analytical tools for deeply nonlinear regime of gravitational collapse [11]. The dynamic evolution of the density correlation function can be predicted based on this hypothesis and pair conservation equation. The hypothesis states that on sufficiently small scales, there is no stream motion between particles in the physical coordinate. In this case, the peculiar motion cancels out the Hubble flow. The hypothesis equivalently states that the mean pairwise peculiar velocity Δu_L (first order

moment) is proportional to the proper separation r between pair of particles, i.e $\langle \Delta u_L \rangle = -Hr$. The structure is bound and frozen and the mean particle separation r (in physical coordinate) is a constant on sufficiently small scales. In this section, the TBCM model is applied to demonstrate the stable clustering hypothesis, which can be extended to high order moments of Δu_L .

The temporal evolution with time scale s can be equivalently transformed to the evolution with physical time t , where $s = t_0 \ln(t/t_i)$ with t_i and t_0 being the initial and current physical time (Eq. (53)). The evolution of comoving size $r_m \propto \exp(-H_0 s) \propto a^{-1}$ for $n = -1$ in the equilibrium range can be obtained from Eq. (40), which means a stable clustering frozen in physical coordinate with a fixed proper separation. The stable clustering is only possible for $n = -1$ in expanding background (Eq. (40)). The peculiar pairwise velocity with equal mass is defined as

$$\Delta u_L(2r) = (\mathbf{u}_1 - \mathbf{u}_2) \cdot \frac{(\mathbf{x}_1 - \mathbf{x}_2)}{|\mathbf{x}_1 - \mathbf{x}_2|}, \quad (113)$$

which can be directly related to the virial quantity $G_s(s)$ derived in Eq. (99). After converting velocity to peculiar velocity with Eq. (6), the pairwise velocity is (from Eq. (72)),

$$a^{1/2} \Delta u_L = \Delta v_L = 2 \frac{\mathbf{r} \cdot \mathbf{v}_1}{r} = 2 \frac{G_s(s)}{r} = 2\dot{r} = \frac{2H_0 r_i}{2+n} \exp\left(\frac{-nH_0 s}{2(2+n)}\right) \cos \theta_s - \frac{2H_0 r}{2+n}, \quad (114)$$

Therefore, for $n = -1$ (using Eq. (74)),

$$\Delta u_L = -\frac{2Har}{2+n} + \frac{2H_0 r_i}{2+n} \cos \theta_s a_i^{\frac{n}{2(2+n)}} a^{\frac{n+1}{n+2}} = -2Har + 2H_0 r_i a_i^{-1/2} \cos \theta_s = -2Har + 2\beta_s u_i \cos \theta_s. \quad (115)$$

Pairs of particles at time a with a separation r can be formed at different initial time a_i with random initial separations r_i and peculiar velocity u_i . Angles θ_s at a given time a can be treated as a random variable (Eq. (67)). Like our treatment of kinetic and potential energies in Eq. (97), the mean peculiar pairwise velocity for many pairs of particles (ensemble average) is

$$\langle \Delta u_L \rangle = -2Har + 2\langle \beta_s u_i \cos \theta_s \rangle. \quad (116)$$

We may safely assume that β_s , u_i , and angle θ_s are independent random variables for a sufficiently large number of pairs. The second term on the RHS of Eq. (116) should vanish as $\langle \cos \theta_s \rangle = 0$. The first order moment of pairwise velocity is therefore proportional to the separation $2r$ for $r \rightarrow 0$ such that

$$\langle \Delta u_L \rangle = -2Har = -2a^{-1/2}H_0r. \quad (117)$$

Equation (117) is often presented as a direct result of stable clustering hypothesis. There have been many attempts to verify this relation with N -body simulations [12, 13], while here we are able to directly demonstrate this result using the TBCM model.

Similar argument can be extended to higher order moments of pairwise velocity. For second order moment, namely the pairwise velocity dispersion, we have (from Eq. (115))

$$\langle \Delta u_L^2 \rangle(r \rightarrow 0) = 4\langle \beta_s^2 u_i^2 \cos^2 \theta_s \rangle > 0 \quad (118)$$

that is dependent on the exact distributions of β_s , u_i , and θ_s . The non-zero pairwise velocity dispersion is an important signature of the collisionless flow, while $\langle \Delta u_L^2 \rangle(r \rightarrow 0) = 0$ for collisional hydrodynamics where pairs of particles are fully correlated with $r \rightarrow 0$. For a uniform distribution of θ_s between $[0, 2\pi]$, $\langle \cos^2 \theta_s \rangle = 1/2$. For particle pairs that will form an equilibrium range (stable clustering), a necessary condition is,

$$\beta_s = \frac{H_0 r_i}{v_i} \leq \beta_{s1} = 1 \quad (119)$$

$$\langle \Delta u_L^2 \rangle(r \rightarrow 0) = 2H_0^2 \langle r_i^2 a_i^{-1} \rangle = 2\langle \beta_s^2 u_i^2 \rangle. \quad (120)$$

The higher order moments of pairwise velocity with $r \rightarrow 0$ can be similarly derived from Eq. (115), where the even and odd moments can be obtained up to the first order of r ,

$$\langle \Delta u_L^{2m} \rangle (r \rightarrow 0) = (2H_0)^{2m} \langle r_i^{2m} \rangle \langle a_i^{-m} \rangle \langle \cos^{2m} \theta_s \rangle, \quad (121)$$

$$\langle \Delta u_L^{2m+1} \rangle (r \rightarrow 0) = -2Har (2H_0)^{2m} \langle r_i^{2m} \rangle \langle a_i^{-m} \rangle \langle \cos^{2m} \theta_s \rangle. \quad (122)$$

A simplified relation is found between the odd and even pairwise velocity moments with $r \rightarrow 0$,

$$\langle \Delta u_L^{2m+1} \rangle = (2m+1) \langle \Delta u_L^{2m} \rangle \langle \Delta u_L \rangle = (2m+1) \langle \Delta u_L^{2m} \rangle (-2Har), \quad (123)$$

which reduces to the standard stable clustering hypothesis (Eq. (117)) for $m = 0$. Equation (123) can be considered as a generalized stable clustering hypothesis for pairwise velocity of any arbitrary order of m .

The $2m$ th order generalized kurtosis of the PDF (Probability Distribution Function) of pairwise velocity Δu_L is defined as,

$$K_{2m} = \langle \Delta u_L^{2m} \rangle / \langle \Delta u_L^2 \rangle^m. \quad (124)$$

Let's assume the second order moment has a general form of $\langle \Delta u_L^2 \rangle = \alpha_u u_0^2 a^{\beta_u}$ when $r \rightarrow 0$, where u_0^2 is the one-dimensional velocity dispersion of the entire N-body system at present epoch. The high order moments and generalized kurtosis of the pairwise velocity for $r \rightarrow 0$ can be obtained as (from Eq. (123)),

$$\langle \Delta u_L^{2m} \rangle = K_{2m} \alpha_u^m u_0^{2m} a^{\beta_u m}, \quad (125)$$

$$\langle \Delta u_L^{2m+1} \rangle = -2(2m+1) K_{2m} \alpha_u^m u_0^{2m+1} a^{\beta_u m - 1/2} (H_0 r / u_0) < 0, \quad (126)$$

$$K_{2m+1}(r) = -2(2m+1) K_{2m} \alpha_u^{-1/2} a^{-(1+\beta_u)/2} (H_0 r / u_0) < 0, \quad (127)$$

where α_u , β_u , and K_{2m} fully determine all these moments. Simulations suggest $\alpha_u = 2$ and $\beta_u = 3/2$. While the limiting one-dimensional velocity follows a X distribution with a Gaussian core and exponential wing [M3], more study is required for the even order kurtosis K_{2m} or the limiting probability distribution of pairwise velocity Δu_L with $r \rightarrow 0$. The TBCM model shows that the odd moments of Δu_L are proportional to r while the even order moments are independent of the separation r when $r \rightarrow 0$.

4.2 Connections with violent relaxation

The violent relaxation is originally proposed for the collisionless system with a time-dependent potential to explain the absence of tendency to segregate different masses during the relaxation [15]. The TBCM model can be considered as a special example of violent relaxation involving only two masses. The evolution of mean separation $r_m(s)$ (Eq. (40)) do not involve particle mass. Particle mass only affects the frequency term $\omega_m(s)$ through initial velocity v_i (Eq. (41)). The characteristic time of relaxation (in scale of s) is only dependent on H_0 , regardless of particle mass (see energy evolution in Eqs. (92) to (97)). Two particles with unequal masses collapse at the same rate with the same characteristic time of relaxation such that this type of relaxation does not lead to mass segregation. We may examine the energy transfer between two particles during a two-body collapse. The initial ratio of kinetic and potential energy between two particles are (from Eqs. (20) and (21) is

$$\frac{K_{si1}}{K_{si2}} = \frac{m_1 v_{1i}^2}{m_2 v_{2i}^2} = \frac{m_1 \mu^2}{m_2 (2 - \mu)^2} = \frac{m_2}{m_1}, \quad \frac{P_{si1}}{P_{si2}} = 1 \quad (128)$$

The kinetic energy of two particles evolves during the two-body collapse is (from Eq. (90)),

$$K_{s1} = \frac{1}{2} m_1 (v_{x1}^2 + v_{y1}^2) = \frac{1}{2} m_1 \mu^2 \left[\dot{r}^2 + r^2 F(s)^{-4} \right], \quad (129)$$

and

$$K_{s2} = \frac{1}{2} m_2 (v_{x2}^2 + v_{y2}^2) = \frac{1}{2} m_2 (2 - \mu)^2 \left[\dot{r}^2 + r^2 F(s)^{-4} \right]. \quad (130)$$

Obviously, the ratio of kinetic energy between two particles is time-invariant and equals the initial ratio in Eq. (128). The potential energy of two particles also evolves with a constant ratio of 1. There is no energy transfer between two particles with unequal mass. The energy equipartition does not apply here. For comparison, during a collisional relaxation, the relaxation time of massive particles is less than that of light particles (inversely proportional to particle mass for a two-body relaxation process [16]). The energy equipartition enables transferring of kinetic energy between particles with massive and light particles sharing the same kinetic energy. Therefore massive particles tend to fall to the center of structure [17].

4.3 Connections with spherical collapse model (SCM)

The spherical collapse model (SCM) solves the motion of spherical shells of matter surrounding an over-density, where many important insights can be obtained for highly-nonlinear gravitationally collapsing objects [3]. This section will reveal some fundamental connections between TBCM and SCM. The equation of motion for a SCM model in physical coordinates reads

$$\frac{d^2 R}{dt^2} = -\frac{GM}{R^2}, \quad (131)$$

where R is the radius of the spherical shell and M is the mass enclosed by that shell. The initial velocity of mass shell is assumed to be Hubble flow,

$$\left. \frac{dR}{dt} \right|_{t=0} = H_i R_i = H_0 x_i a_i^{-1/2} \quad (132)$$

where $x_i = x(t=0)$ is the initial radius in a comoving system. Solution to Eq. (131) can be written in a parametric form,

$$R = A(1 - \cos \theta) \text{ and } t = B(\theta - \sin \theta), \quad (133)$$

where two constants A and B are related to the initial radius x_i in comoving coordinates,

$$x_i = x(t=0) = A(12\pi)^{2/3} / 2 \text{ and } A^3 = GMB^2. \quad (134)$$

For a direct comparison, the SCM model (Eq. (131)) can be equivalently expressed in the transformed system with comoving coordinate x and time scale s ,

$$\frac{\partial^2 x}{\partial s^2} + \frac{H_0}{2} \frac{\partial x}{\partial s} + \frac{GM}{x^2} = \frac{H_0^2}{2} x. \quad (135)$$

By setting $x = 2r$ (SCM models a spherical over-density with uniform mass distribution), the SCM Eq. (135) can be rewritten as

$$\frac{\partial^2 r}{\partial s^2} + \frac{H_0}{2} \frac{\partial r}{\partial s} + \frac{GM}{2(2r)^2} = \underbrace{\frac{H_0^2}{2}}_1 r. \quad (136)$$

The TBCM model presented in Section 3.1 (Eq. (30)) describes a two-body system in an expanding background with uniform density. The equation reads

$$\frac{\partial^2 r}{\partial s^2} + \frac{H_0}{2} \frac{\partial r}{\partial s} + \frac{GM}{2(2r)^2} = \underbrace{\frac{(r_i v_i)^2}{r^3}}_2 \exp(-H_0 s), \quad (137)$$

where $M = m_1 + m_2$ is the total mass of two-body system. The SCM model essentially describes a self-gravitating system in an otherwise empty universe (Eq. (131)). The energy is conserved for SCM model in physical coordinates. By comparing the SCM Eq. (136) with the TBCM Eq. (137), the original SCM model has an extra force term on the RHS (term 1 in Eq. (136)) that is due to

the absence of a uniform background density. The TBCM model has a time-varying frequency force due to the angular momentum (term 2 in Eq. (137)).

The original SCM can be considered to describe exactly a two-body collapse in an otherwise empty universe, with one-dimensional radial motion only and zero angular momentum. The initial conditions for original SCM model (Eq. (136)) is an initial separation $r_i = x_i/2$ (Eq. (134)) and a zero initial velocity in a transformed system. The modified non-radial SCM model introduces an additional constant centrifugal force to indirectly account for the effect of non-radial motion [7, 8], while it still models a self-gravitating system in an otherwise empty universe.

Equivalently, the proposed TBCM model in expanding background can be considered as a spherical non-radial collapse model describing the gravitational collapse of a mass shell with a non-zero angular momentum and non-radial orbits (non-radial spherical collapse model). Both models predict a critical halo density ratio of $\Delta = 18\pi^2$ to the background density. However, the original SCM model cannot predict the existence of an equilibrium range (stable clustering for $n = -1$). In SCM model, the system is out of virial equilibrium initially and reaching the virial equilibrium at the critical density, where effect of halo mass accretion is not explicitly considered.

For comparison, the TBCM model allows the existence of an equilibrium range for $\beta_s \leq \beta_{s1}$, where the initial density is at least twice the background density (Eqs. (78) and (87)). The TBCM model can be considered as the elementary step for mass accretion/cascade. Halos with an infinitesimal lifetime (due to the fast mass accretion) approach a critical density with a ratio of $\Delta = 18\pi^2$ to the background, where β_s converges to the critical value $\beta_{s2} = 1/3\pi$ (Eqs. (82) and (87)). The stable clustering hypothesis can be demonstrated by the TBCM model and generalized to high order moments of pairwise velocity. Rich information on halo energy/momentum/structure can be obtained from a TBCM model.

5. Conclusion

A transformed equation system is proposed by introducing a different time scale s for the motion of collisionless particles in expanding background (Eq. (5)). The equivalence with the original comoving systems is established. A two-body collapse model (TBCM) for gravity with an arbitrary exponent n is formulated in the transformed system (Eq. (11)). Results obtained can be readily translated back to the original system. A complete analysis of TBCM model is provided with governing equations for radius function (Eq. (30)) or frequency function (Eq. (34)). The original five model parameters, i.e. the potential exponent n , Hubble constant H_0 , initial size r_i and velocity v_i , and system mass $M = m_1 + m_2$, can be grouped into three dimensionless parameters n , $\beta_s = H_0 r_i / v_i$, and $\gamma_s = (v_{ri} / v_i)^2$ (Eqs. (60), (61) and Table 1). Here v_{ri} is the circling velocity for a given r_i and M , and n in static background without damping. The competition between gravitational force, expanding background (damping), and angular momentum classifies the two-body collapse into two categories (Fig. 5): 1) a free fall collapse without oscillatory motion for weak angular momentum; and 2) an equilibrium collapse with oscillations for weak damping, when $\beta_s \ll 1$, $-2 < n < 0$ and $\gamma_s \sim 1$.

For free fall collapse, the free fall time t_c in an expanding background can be analytically derived as a function of the free fall time s_{ce} in static background and the beginning time t_i of free fall (Fig. 7 and Eq. (57)). The two-body collapse can have a greater free fall time t_c if two-body system begins to collapse at an earlier time t_i .

For an equilibrium collapse, solutions identify three distinct regimes (transitional, equilibrium, and final collapse in Fig. 5). An exponential evolution of two-body system size, energy and

momentum can be obtained in transformed system (Fig. 4, Eqs. (76), (92), (93), (94), (99) and (100)), or equivalently a power-law evolution in the original comoving system. A critical value of $\beta_s \leq \beta_{s1}$ (Eq. (78)) is required for the existence of an equilibrium range. Equivalently, a maximum system size or a minimum initial velocity can be identified (Eq. (79)). The second critical value of $\beta_s = \beta_{s2}$ (Eq. (82)) can be identified for large halos with an infinitesimal lifetime (due to fast mass accretion). Large halos tend to be synchronized and generated at the same time with small dispersion in their properties. Conversely, small halos tend to have longer lifetime with more diversified properties at a given redshift. The two-body angular velocity (Eq. (103)), typical orbital period (Eq. (85)), the ratio between radial and circular motion (Eq. (104)), and the critical density ratio of $18\pi^2$ (Eq. (89)) can all be derived from the TBCM model. Isothermal density profile is also a direct result of an infinitesimal lifetime

Finally, the TBCM model demonstrates the stable clustering hypothesis (SCH) for an equilibrium collapse, where mean pairwise velocity is proportional to separation (Eqs. (114) and (117)). A generalized stable clustering hypothesis (GSCH) is also developed for higher odd and even order moments that are related by mean pairwise velocity (Eqs. (121), (122) and (123)). The two-body collapse in expanding background is independent of particle masses, where the energy equipartition does not apply. Compared to the original spherical collapse model (SCM), the TBCM model can be naturally considered as a spherical non-radial collapse model with non-zero angular momentum (Eqs. (136) and (137)). Both models predict the same critical halo density ratio of $18\pi^2$, while the original SCM model cannot predict a stable clustering. The TBCM model also suggests a power-law energy evolution at large scale that will be further investigated.

Reference

1. Xu, Z., *Inverse mass cascade of self-gravitating collisionless flow and effects on halo mass functions*. arXiv:2109.09985 [astro-ph.CO], 2021.
2. Xu, Z., *The maximum entropy distributions of collisionless particle velocity, speed, and energy for statistical mechanics of self-gravitating collisionless flow (SG-CFD)*. arXiv:2110.03126 [astro-ph.CO], 2021.
3. Gunn, J.E. and J.R. Gott, *Infall of Matter into Clusters of Galaxies and Some Effects on Their Evolution*. *Astrophysical Journal*, 1972. **176**(1): p. 1-8.
4. Gunn, J.E., *Massive Galactic Halos .1. Formation and Evolution*. *Astrophysical Journal*, 1977. **218**(3): p. 592-598.
5. Fillmore, J.A. and P. Goldreich, *Self-Similar Gravitational Collapse in an Expanding Universe*. *Astrophysical Journal*, 1984. **281**(1): p. 1-8.
6. Bertschinger, E., *Self-Similar Secondary Infall and Accretion in an Einstein-DeSitter Universe*. *Astrophysical Journal Supplement Series*, 1985. **58**(1): p. 39-66.
7. White, S.D.M. and D. Zaritsky, *Models for Galaxy Halos in an Open Universe*. *Astrophysical Journal*, 1992. **394**(1): p. 1-6.
8. Nusser, A., *Self-similar spherical collapse with non-radial motions*. *Monthly Notices of the Royal Astronomical Society*, 2001. **325**(4): p. 1397-1401.
9. Peebles, P.J.E., *The gravitational instability picture and the nature of the distribution of galaxies*. *The Astrophysical Journal*, 1974. **189**: p. L51-L53.
10. Davis, M. and P.J.E. Peebles, *Integration of Bbgky Equations for Development of Strongly Nonlinear Clustering in an Expanding Universe*. *Astrophysical Journal Supplement Series*, 1977. **34**(4): p. 425-450.
11. Peebles, P.J.E., *The Large-Scale Structure of the Universe*. 1980, Princeton, NJ: Princeton University Press.
12. Efstathiou, G., et al., *Gravitational Clustering from Scale-Free Initial Conditions*. *Monthly Notices of the Royal Astronomical Society*, 1988. **235**(3): p. 715-748.
13. Colombi, S., F.R. Bouchet, and L. Hernquist, *Self-similarity and scaling behavior of scale-free gravitational clustering*. *Astrophysical Journal*, 1996. **465**(1): p. 14-33.
14. Xu, Z., *Inverse mass cascade of self-gravitating collisionless flow and effects on halo deformation, energy, size, and density profiles*. arXiv:2109.12244 [astro-ph.CO], 2021.
15. Lyndenbell, D., *Statistical Mechanics of Violent Relaxation in Stellar Systems*. *Monthly Notices of the Royal Astronomical Society*, 1967. **136**(1): p. 101-+.
16. Leigh, N., A. Sills, and T. Boker, *Modifying two-body relaxation in N-body systems by gas accretion*. *Monthly Notices of the Royal Astronomical Society*, 2013. **433**(3): p. 1958-1965.
17. Spitzer, L., Jr., *Equipartition and the Formation of Compact Nuclei in Spherical Stellar Systems*. *Astrophysical Journal*, 1969. **158**.

Supplementary information for
Non-radial two-body collapse model (TBCM) in expanding background
and generalized stable clustering hypothesis (GSCH)

Zhijie Xu^{1,a}

1. Computational Mathematics Group, Physical and Computational Sciences Directorate, Pacific
Northwest National Laboratory, Richland, WA 99352, USA

a) Electronic mail: zhijie.xu@pnnl.gov; zhijiexu@hotmail.com

Symbol	S.I. Unit	Physical Meaning
Ω_0	Dimensionless	Matter content
Λ	$1/m^2$	Universe constant
h	Dimensionless	Dimensionless Hubble constant
Γ	Dimensionless	$\Gamma = \Omega_0 h$ Shape parameter for power spectrum
σ_8	Dimensionless	Density fluctuation at $r = 8Mpc/h$
L	m	Size of simulation box
N	Dimensionless	Number of particles in the simulation
m_p	kg	Mass of collisionless particle
l_{soft}	m	Gravitational soften length
V	m^3	Volume of simulation box
b	Dimensionless	Linking length parameter
n	Dimensionless	Exponent of the particle-particle interaction potential. Specifically, $n = -1$ represents the gravitational interaction.
G_n, G	$m^{2-n}/(kg \cdot s^2)$	Gravitational constant for arbitrary n and for $n=-1$
$V_p(r)$	m^2/s^2	Two-body potential energy as a function of distance particle r
a, z	Dimensionless	Scale factor and redshift
H_0, H	$1/s$	Hubble constants ('0' stands for current epoch)
t_0, t, t_i	s	Physical time (subscript '0' for current epoch and 'i' for initial)
s	s	Transformed time scale such that $ds/dt = a^p$
$\bar{\rho}_y(a)$	kg/m^3	Physical background density at scale factor a
$\mathbf{x}_i, \mathbf{r}_i$	m	Position vector in comoving and physical coordinates
$\mathbf{F}_i, \mathbf{F}_{ij}$	$kg \cdot m/s^2$	The total force for particle i , and the force between pair of particles i and j
$\mathbf{v}_i = d\mathbf{x}_i/ds$	m/s	The transformed velocity of particle i in transformed system
$\mathbf{u}_i = a d\mathbf{x}_i/dt$	m/s	The peculiar velocity vector of collisionless particle i
K_s, K_p	m^2/s^2	Specific kinetic energy of transformed and peculiar velocities
ω_s	$1/s$	Angular velocity of two-body system
P_s, P_y	m^2/s^2	Specific potential energy in comoving and physical coordinates
E_s, E_y	m^2/s^2	Specific total energy in the transformed and comoving systems

V_y	m^2/s^2	The virial energy defined as $2K_p - nP_y$
G_s, G_p	m^2/s	Specific virial quantity in transformed and comoving systems
$\mathbf{H}_s, \mathbf{H}_p$	m^2/s	Specific angular momentum in transformed and comoving systems
$u_0^2, u^2(a)$	m/s	The one-dimensional velocity dispersion as a function of a
γ	Dimensionless	Scaling exponent with $u^2(a) \propto a^\gamma$
\mathbf{R}	m	The position vector of the center of mass
$\mathbf{r}, r(s)$	m	The displacement vector and the magnitude
\mathbf{v}	m/s	Velocity of the displacement vector \mathbf{r}
$\theta_{\mathbf{vr}}$	Dimensionless	The angle between vectors \mathbf{r} and \mathbf{v}
m_1, m_2	kg	Two masses of the two-body problem
$\mathbf{x}_1, \mathbf{x}_2$	m	Position vectors of two masses
$\mathbf{v}_1, \mathbf{v}_2$	m/s	Velocity vector of two masses
μ	Dimensionless	Ratio between two masses
$\omega(s)$	$1/s$	Frequency for the motion of the displacement vector
$\mathbf{x}_{i1}, \mathbf{x}_{i2}$	m	Initial position vectors of two masses at $s=0$
\mathbf{r}_i, r_i	m	Initial position of the displacement vector and the magnitude
\mathbf{v}_i, v_i	m/s	Initial velocity of the displacement vector and the magnitude
v_{i1}, v_{i2}	m/s	Initial speed of two masses
v_{ri}	m/s	The circular speed of the displacement vector \mathbf{r} without damping
$M = m_1 + m_2$	kg	Total mass of the two-body system
$F(s)$	$s^{1/2}$	Frequency function introduced to solve the two-body collapse
$\gamma_s = (v_{ri}/v_i)^2$	Dimensionless	Ratio of circling velocity v_{ri} to the initial velocity v_i
$\lambda_s = H_0 r_i / (4v_i)$	Dimensionless	Parameter for the competition between gravitational interaction and expanding background
$\lambda_{si} = H_0 r_i / (4v_{ri})$	Dimensionless	$\lambda_{si} = \lambda_s$ if $v_i = v_{ri}$
s_t	s	The critical time for transitional period
s_c	s	The free fall time in a transformed system
s_{c1}	s	The free fall time for small λ_{si} in a transformed system
s_{c2}	s	The free fall time for large λ_{si} in a transformed system

s_{ce}	s	The exact free fall time in a static background without damping
t_e	s	The physical time at the end of a free fall
t_c	s	The elapsed physical time of a free fall
$F_m(s)$	$s^{1/2}$	Mean solution of the frequency function $F(s)$
$r_m(s)$	m	Mean solution of the radius $r(s)$
$\omega_m(s)$	$1/s$	Mean solution of the angular frequency $\omega(s)$
$F_a(\omega_m s)$	Dimensionless	The amplitude of the frequency function $F(s)$
$k_s(n, \gamma_s)$	Dimensionless	The frequency function of the oscillation solution
$\theta_s(\omega_m s)$	Dimensionless	The angle function of the oscillation solution
α_s	Dimensionless	The virial constant
$\beta_s = H_0 r_i / v_i$	Dimensionless	Parameter quantifying the competition between gravitational attraction and expanding background
β_{s1}	Dimensionless	Critical value of β_s to form the equilibrium range
β_{s2}	Dimensionless	Critical value of β_s to form the equilibrium range from $t = 0$
r_{ic} and v_{ic}	m and m/s	Critical radius and velocity to form the equilibrium range
T_s	s	The period of the two-body gravitational collapse
$\rho_y(t), \rho_s(t)$	kg/m^3	The halo density in physical and comoving coordinates
r_h, r_g	m	The comoving halo radius (size) and mean square radius
K_h, P_h	m^2/s^2	Halo peculiar kinetic energy and potential energy
$\sigma_v^2 = 2K_h/3$	m^2/s^2	Halo one-dimensional velocity dispersion
n_p	Dimensionless	The number of particles in a given halo
\mathbf{v}_h	m/s	Halo velocity
$\rho_h(r)$	kg/m^3	Halo density profile as a function of distance r
c	Dimensionless	The concentration parameter for NFW halo density profile
r_{vir}	m	The halo virial radius for NFW density profile
α_s^*, β_s^*	Dimensionless	Halo parameters computed from simulation
z_s^*, n_s^*	Dimensionless	Halo ratio constant and potential exponent
τ_s^*, η_s^*	Dimensionless	Halo parameters defined for halo virial quantity and halo angular momentum
τ_{s1}^*, η_{s1}^*	Dimensionless	Proportional constants defined for halo virial quantity and halo angular momentum
N_h	Dimensionless	Number of halos in the entire system

$\mathbf{x}_h, \mathbf{x}'_p$	m	Position vector of the halo center of mass and particle position vector relative to the halo center of mass
$\mathbf{u}_h, \mathbf{u}'_p$	m/s	Halo velocity vector and the particle velocity vector relative to the halo velocity
$\mathbf{H}_h, \mathbf{H}_e$	m^2/s	Angular momentum from the random motion of particles in halo and motion of the halo, respectively
G_h, G_e	m^2/s	Virial quantity from the random motion of particles in halo and motion of the halo, respectively
θ_h	Dimensionless	The mean angle between \mathbf{u}'_p and \mathbf{x}'_p for every halo
σ_h^2	m^2/s^2	One-dimensional halo velocity dispersion for halos of the same size
Δu_L	m/s	Pairwise velocity
α_u, β_u	Dimensionless	Parameters modeling the pairwise velocity dispersion $\langle \Delta u_L^2 \rangle$
R	m	The radius of the spherical top-hat overdensity
α, β	Dimensionless	Parameters for kinetic and potential energy evolution
ε_u	m^2/s^3	The energy production rate of self-gravitating collisionless fluid flow